NAVAL POSTGRADUATE SCHOOL
Monterey, California

THESIS

GENETIC ALGORITHM DESIGN AND TESTING OF A RANDOM ELEMENT 3-D 2.4 GHZ PHASED ARRAY TRANSMIT ANTENNA CONSTRUCTED OF COMMERCIAL RF MICROCHIPS

by

Lance C. Esswein

June 2003

Thesis Advisor:	Michael Melich
Co-Advisor:	David Jenn
Co-Advisor:	Rodney Johnson

THIS PAGE INTENTIONALLY LEFT BLANK

REPORT DOCUMENTATION PAGE		Form Approved OMB No. 0704-0188

Public reporting burden for this collection of information is estimated to average 1 hour per response, including the time for reviewing instruction, searching existing data sources, gathering and maintaining the data needed, and completing and reviewing the collection of information. Send comments regarding this burden estimate or any other aspect of this collection of information, including suggestions for reducing this burden, to Washington headquarters Services, Directorate for Information Operations and Reports, 1215 Jefferson Davis Highway, Suite 1204, Arlington, VA 22202-4302, and to the Office of Management and Budget, Paperwork Reduction Project (0704-0188) Washington DC 20503.

1. AGENCY USE ONLY *(Leave blank)*	2. REPORT DATE June 2003	3. REPORT TYPE AND DATES COVERED Master's Thesis
4. TITLE AND SUBTITLE Genetic Algorithm Design And Testing Of A Random Element 3-D 2.4 Ghz Phased Array Transmit Antenna Constructed Of Commercial Rf Microchips		5. FUNDING NUMBERS
6. AUTHOR (S) Lance C. Esswein		
7. PERFORMING ORGANIZATION NAME(S) AND ADDRESS(ES) Naval Postgraduate School Monterey, CA 93943-5000		8. PERFORMING ORGANIZATION REPORT NUMBER
9. SPONSORING / MONITORING AGENCY NAME(S) AND ADDRESS(ES)		10. SPONSORING/MONITORING AGENCY REPORT NUMBER

11. SUPPLEMENTARY NOTES The views expressed in this thesis are those of the author and do not reflect the official policy or position of the U.S. Department of Defense or the U.S. Government.

12a. DISTRIBUTION / AVAILABILITY STATEMENT Approved for public release; distribution is unlimited.	12b. DISTRIBUTION CODE

13. ABSTRACT *(maximum 200 words)*

The United States Navy requires radical and innovative ways to model and design multi-function phased array radars. This thesis puts forth the concept that Genetic Algorithms, computer simulations that mirror the natural selection process to develop creative solutions to complex problems, would be extremely well suited in this application. The capability of a Genetic Algorithm to predict adequately the behavior of an array antenna with randomly located elements was verified with expected results through the design, construction, development and evaluation of a test-bed array. The test-bed array was constructed of commercially available components, including a unique and innovative application of a quadrature modulator microchip used in commercial communications applications. Corroboration of predicted beam patterns from both Genetic Algorithm and Method of Moments calculations was achieved in anechoic chamber measurements conducted with the test-bed array. Both H-plane and E-plane data runs were made with several phase steered beams. In all cases the measured data agreed with that predicted from both modeling programs. Although time limited experiments to beam forming and steering with phase shifting, the test-bed array is fully capable of beam forming and steering though both phase shifting and amplitude tapering.

14. SUBJECT TERMS Bi-Static Radar, Active, Phased Array, Antenna, Radar, Radar Design, Air Search Radar, Evolutionary Computation, Genetic Programming, Genetic Algorithms, Theater Ballistic Missile Defense (TBMD), Area Air Defense, Air Warfare.			15. NUMBER OF PAGES 135
			16. PRICE CODE
17. SECURITY CLASSIFICATION OF REPORT Unclassified	18. SECURITY CLASSIFICATION OF THIS PAGE Unclassified	19. SECURITY CLASSIFICATION OF ABSTRACT Unclassified	20. LIMITATION OF ABSTRACT UL

NSN 7540-01-280-5500

Standard Form 298 (Rev. 2-89)
Prescribed by ANSI Std. 239-18

THIS PAGE INTENTIONALLY LEFT BLANK

**GENETIC ALGORITHM DESIGN AND TESTING OF A RANDOM ELEMENT
3-D 2.4 GHZ PHASED ARRAY TRANSMIT ANTENNA
CONSTRUCTED OF COMMERCIAL RF MICROCHIPS**

Lance C. Esswein
Lieutenant Commander, United States Navy
B.S., California State University at Fresno, 1988

Submitted in partial fulfillment of the
requirements for the degree of

MASTER OF SCIENCE IN PHYSICS

from the

**NAVAL POSTGRADUATE SCHOOL
June 2003**

Author: Lance C. Esswein

Approved by: Michael Melich
                 Thesis Advisor

                 David Jenn
                 Co-Advisor

                 Rodney Johnson
                 Co-Advisor

                 William B. Maier II
                 Chairman, Department of Physics

iii

THIS PAGE INTENTIONALLY LEFT BLANK

ABSTRACT

The United States Navy requires radical and innovative ways to model and design multi-function phased array radars. This thesis puts forth the concept that Genetic Algorithms, computer simulations that mirror the natural selection process to develop creative solutions to complex problems, would be extremely well suited in this application. The capability of a Genetic Algorithm to predict adequately the behavior of an array antenna with randomly located elements was verified with expected results through the design, construction, development and evaluation of a test-bed array. The test-bed array was constructed of commercially available components, including a unique and innovative application of a quadrature modulator microchip used in commercial communications applications. Corroboration of predicted beam patterns from both Genetic Algorithm and Method of Moments calculations was achieved in anechoic chamber measurements conducted with the test-bed array. Both H-plane and E-plane data runs were made with several phase-steered beams. In all cases the measured data agreed with that predicted from both modeling programs. Although time limited experiments to beam forming and steering with phase shifting, the test-bed array is fully capable of beam forming and steering though both phase shifting and amplitude tapering.

THIS PAGE INTENTIONALLY LEFT BLANK

TABLE OF CONTENTS

LIST OF FIGURES

THIS PAGE INTENTIONALLY LEFT BLANK

LIST OF TABLES

THIS PAGE INTENTIONALLY LEFT BLANK

ACKNOWLEDGEMENTS

They that go down to sea in ships, that do business in great waters: These see the works of the Lord, and his wonders in the deep.

107th Psalm

THIS PAGE INTENTIONALLY LEFT BLANK

I. INTRODUCTION

A. MOTIVATION

Naval warfare evolves under the pressure of new missions, new operational environments and newly applied technology. While a warship's ability to put ordnance on target in an accurate and timely manner has remained constant, the targets, the ordnance and notions of accuracy and timeliness have changed radically from the days of sail, as the swords and muskets of yesteryear gave way to stealth cruise missiles and the AEGIS combat systems of today. This thesis asks if the combination of widely available, inexpensive radio frequency (RF) semiconductors, high performance computers, evolutionary computation, and the growing needs of ballistic missile defense for more exacting identification of detected objects, can come together to produce a radical improvement in affordable warship sensor performance. In particular, can cellular phone transmit chips, configured randomly in three dimensions, produce the transmit beams predicted by beam forming computer codes based on genetic algorithms? The short answer presented here is a resounding YES.

The implications for future warship design include:

- Full exploitation of the 150-200m size of warships for antenna apertures, which could lead to high resolution radars at VHF/UHF frequencies that may be competitive with X-band Cobra series radars for space tracking.

- Lowered single-point-of-failures vulnerabilities compared to previous radars, such as AEGIS AN/SPY-1.

- New topside antenna designs, where antennas for all combat system functions including a full range of communications, signal intercept, fire control, search and track, etc., are integral or conformal to the ship's hull.

- New design opportunities for reducing the ship's RF and IR signatures when coupled to the flexibility promised by electrical propulsion.

- Realization of the oft-promised proportional reduction in cost, as performance requirements are proportionately reduced, because the performance of the phased array discussed in this thesis is directly proportional to the number of Transmit/Receive elements bought, installed, and operated.

1.   What is Happening in Warship Design Today?

The Navy has not built a revolutionary surface warship design since the introduction of the AEGIS fleet, and that was based on a conventional existing hull. The AEGIS combat system architecture and implementation constraints technologically belong in the late 1960's and early 1970's. The quality of the system architecture has proven to be a sturdy foundation for the evolution and growth that has been seen over the last 25 years. But as RADM Wayne E. Mayer, the Father of AEGIS, observed in the early 1990's, AEGIS is 25 years old, conceptually, and the future fleet must be grounded

in the technological opportunities of today, not 1965, or 1995 for that matter, to meet the missions of the first half of the twenty-first century. AEGIS, the Navy's primary answer to the cruise missile threat created by the former Soviet Union, had the effect of extending the effective life of carrier task forces. The issue for today, still under intense debate, is what should the future fleet be designed to do? There are the champions for the carrier battle groups and crusaders for clusters of small ships closely coupled to build aggregate sensor and firepower capability comparable to that of most existing combatants. The issue is far from settled. The pressure from the current administration in the Department of Defense (DoD) is for "transformation", not just reform. That means, a paradigm shift in what we are doing and not just a marginal improvement.

The work presented in this thesis offers a technology that can make possible combatant designs that support the most critical mission areas.

2.   Revolutionary Solution

What if the radar could be designed on the ideal ship architecture instead of designing the ship around radar, which is a current AEGIS situation? If the ship's structure minimized radar cross-section and maximized survivability and maneuverability, and the ships sensor systems were molded into this shape, the ship would break the paradigm of current naval architecture. What if these radiating elements could serve as both radar and communications links, eliminating the seemingly hundreds of masts and antennas populating current ship

superstructures? What if the entire length of the ship were made the array aperture? Target resolution would be increased magnitudes. For example: the typical AEGIS radar is roughly 4 meters across operating frequency (n) at roughly 3GHz. This provides a base wavelength (l) of 10 centimeters or 1/10 of a meter. If instead, the array were the entire length of the AEGIS cruiser, roughly 200 meters, operating on the same frequency and wavelength, the resolution would be increased 50 times. This could allow for the radar to image threats. Although there are current imaging radars in the fleet today (ISAR, SAR, SARTIS, NCTR), the systems require high frequency radar lock-on emulating fire control solutions. The target may assume this is hostile intent or hostile act to retaliate accordingly. The new high-resolution radar would alleviate this confusion in would not violate rules of engagement (ROE).

Alternatively, frequency could be greatly reduced while maintaining the same resolution. The advantages of using VHF/UHF wavelengths include longer range detection, reduced counter-detection, and anti-stealth or stealth defeating detection.

The purpose of this thesis is to show that Genetic Algorithms are capable of designing random element phase arrays. Phase One was the topic of "Genetic Algorithms as a Tool for Phased Array Radar Design", Master's Thesis by Jon A. Bartee, LT, USN, June 2002. In this phase, a passive or receive array of 24 elements was used to verify initial genetic algorithms capabilities and possibilities. Phase Two, the subject of this thesis, is to assess whether the Genetic Algorithm works as a design and beam-forming tool for active

4

or transmitting phase arrays. Additional thesis objectives were to use silicon based commodity microprocessors to evaluate the possibilities of using these components and future radars and communication applications.

The process of using genetic algorithms in radar design has many advantages. Running a series of genetic algorithm programs can determine the evolved array configuration that is compatible with the naval architect's design criteria. The initial Phase One project dealt with a two-dimensional planar radar. Phase Two employs a three-dimensional radar, proving the robust capability of the GA, allowing the naval architect to place elements based on optimal solutions and not restricted to traditional design concepts. The algorithm can choose available locations provided by the naval architect after vital services are in place; basically where convenient, instead of plumbing services based on radar location. Genetic algorithms have no favoritism, no loyalty, and no inclination toward a previous solution in order to predict the best solution or the desired solution. The solution generated is one presented based on optimal performance. Additionally, due to variably spaced element locations, survivability is increased. For example: an AEGIS cruiser in a shipyard overseas on a deployment had catastrophic failure to one of its arrays when a shipyard crane hit the array face. This destroyed one quadrant of the radar surveillance and engagement capability. With multitudes of elements spaced throughout the entire construction of the ship, damage to a few elements would have a minimal impact on radar performance.

B.   SCOPE AND ORGANIZATION

1.   Scope

This Phase Two thesis will test a Genetic Algorithm program called "EXTHIN5.m". The performance measurements were taken on an active phased array radar antenna constructed entirely with commodity available "off-the-shelf" hardware. The program code tested was one that constructs the antenna patterns and calculates the effectiveness of the solution.

2.   Primary Research Questions

a.   Is it feasible to build a phased array radar with readily available commercial/commodity components?

b.   Can the EXTHIN5.M Genetic Algorithm (GA) code actually beam form for digital phased array radar operations including thinned, distributed, disjoint and reconfigurable aperture geometries?

3.   Organization

Chapter II is a discussion of computational analysis for Genetic Algorithms. Population design is discussed and the coordinate system used is explained. Specification of the fitness criterion used and the genetic operations performed is described. The decision making process is then illustrated through the use of the actual EXTHIN5.m code using parameter values that were utilized in the design of this active phased array radar. A walk though of the programming decision making

process is conducted and a review and summary of all GA runs is presented.

Chapter III lays out the experimental objectives to determine the effectiveness of the GA as a radar design tool, and discusses the following topics: goals and objectives; radar component selection, design and construction; instrumentation for measurement and evaluation; description of antenna array component selection and construction including component verification and calibration, subassembly test and verification; a detailed discussion on the anechoic chamber antenna measurements and evaluation; and a summary the experimental results achieved with error analysis.

Chapter IV discusses the conclusions made in this thesis and recommendations for follow-on research projects and objectives.

Appendix A is the glossary of terms and abbreviations used within this thesis.

Appendix B is basic genetic algorithm theory and is an excerpt from "Genetic Algorithms as a Tool for Phased Array Radar Design", Master's Thesis by Jon A. Bartee, LT, USN, June 2002.

Appendix C displays an inventory of the major components used to build the radar.

Appendix D provides the active phased array element locations in the XYZ plane for this thesis experiment.

7

Appendix E contains the Master Equipment Configuration and all sub-system schematics.

Appendix F lists PIN-OUTS for the various AD8346EVAL CCA control signal cables at the terminal block interface.

Appendix G lists the OFFSET's required for the LabVIEW program ConversionFinal.vi, which equate to the measured path length error for each of the twenty-four elements.

Appendix H defines the cable numbering convention used in this project.

II. GENETIC ALGORITHMS

A.   USING COMPUTATIONAL ANALYSIS FOR GENETIC SELECTION

Survival of the fittest: Darwin's theories of nature's rules of natural selection have been the topic of numerous studies in all areas of science. Families of biological organisms improve their ability to survive through a generational process of optimization. Evolutionary processes occur in biological systems when the organism has the ability to reproduce itself, there is a population of such organisms, there is variety among the members of the population and that variety can be related to the ability to survive in the environment.[1] Through reproduction and breeding, superior survival traits can be maximized in each successive generation, while undesirable characteristics can be reduced and even eliminated over time. Individuals in a population that are the best suited to survive generally receive favorable treatment in the reproductive process; but note, not only the best-suited individuals produce offspring. A population's vitality depends on its genetic variety or diversity just as much as on the superior individuals. Without this mixture of traits within the population, adaptation to the continuously changing environment would cease and the population eventually stagnates.

Genetic Algorithms work along similar lines to optimize other systems at a higher rate and at a lower cost versus undirected "trial and error" methods of production or evaluation. With the computer's ability to do millions or

billions of repetitive calculations at ultra-high speed, it is now possible to replicate the outcome of hundreds of generations in a reasonable time. The true challenge is modeling what process or outcome is desired though genetic algorithms. In developing the program, or "code", it is necessary to determine what the problem is and how it can be put into a program in a form for exploration by a digital processor.

A review of basic genetic algorithm theory (an excerpt from Bartee) is included as Appendix B for those not familiar with Phase One of the project and the Genetic Algorithm process.

B. THE EXTHIN5.M CODE

Certain aspects of the Genetic Algorithm (GA) code must be discussed in order to fully understand the thought process involved in designing the EXTHIN5.m code. Only then can the application of this code to phased array radar design be understood. Written in MATLAB[2] programming language, EXTHIN5.m was developed by Dr. Rodney Johnson of the United States Naval Postgraduate School. The EXTHIN5.m program is proprietary and not contained within this thesis. Questions regarding the code should be directed to Professor Rodney Johnson. The code was tailored to the problem of beam-shaping/beam-forming and steering using phase shifts and, potentially, amplitude tapering on an active phased array radar with arbitrarily positioned elements.

1. Population Design

Each individual population member is characterized by physical radar design parameters: an amplitude and phase for each array element. For phase-only beam forming, each "amplitude" is a single bit: "on" or "off". The Genetic Algorithm chooses values for these parameters to evolve antenna patterns, selecting those that maximize a given "fitness" criterion. In the work reported here, the criterion was the ratio of the main beam peak to average sidelobe level. The EXTHIN5.m code was designed to show that antenna patterns similar or superior to those obtained by conventional methods could be formed, sometimes even using fewer elements.

In experiments with a predecessor to EXTHIN5.m, a thinned $10l \times 10l$ array was used. A fully populated array of that size has 400 elements spaced at $l/2$ intervals. These were replaced with 100 elements randomly located in the same $10l \times 10l$ area.

For comparison, an antenna pattern was computed for a boresight beam dead center and normal to the array surface, with all elements active or "on" and all phases set to zero. Figure 1 on page 13 displays the results of the above case versus the GA's improved performance. The GA was able to thin the array by 17 elements or 17 percent, while providing the same or increased radar performance exemplified by the peak main lobe to average sidelobe ratio. Turning unnecessary elements off, and compensating for them with phase shifts from the other elements achieved this result.

Herein lies the problem: which elements can be turned off? This unusual determination is part of the unique nature of the GA. An engineer, through years of experience, might be able to thin the array, but it would be through "trial and error" involving tremendous laboratory and time resources. Even then, the final result may not be the best, since all permutations may not have been fully realized or even explored. It is this fact that allows the GA to realize its full potential as a design tool.

Without verification, one cannot be assured EXTHIN5.m is a valid design tool. Phase One explored a 7.6GHz two dimensional, passive or receive array with 24 elements and phase shifting only. Phase Two was selected to demonstrate the EXTHIN5.m code using a 2.4GHz, three dimensional, active phased array antenna with phase shifting and possible amplitude tapering. The number of elements remained at 24 as a result of cost and fabrication considerations.

Element locations were selected using random numbers. The GA thus seeks the best patterns subsequent to selection of these element locations. Each of the elements has two data parameters: amplitude and phase. Initially, amplitude was either "on" or "off". Later, through amplitude tapering, specific values of amplitude can be used. Each antenna pattern is defined by forty-eight unique data elements.

Figures 1 and 2 display the results from the earlier GA program for the 100-element planar array of size $10\lambda x10\lambda$. Three successive runs were completed, with varied GA parameters. The population was set at 5000 members. The

distribution of the initial population for the first run was randomly determined, while the subsequent two runs were each seeded with the results from the previous run.
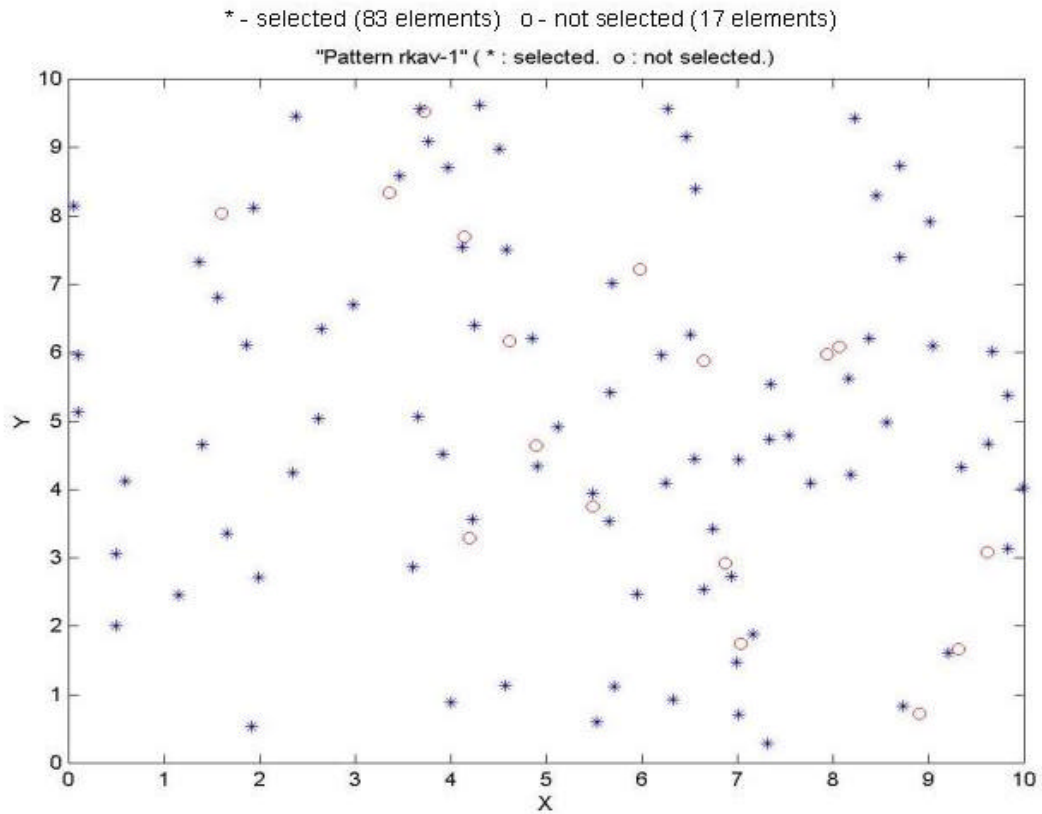
Figure 1:   One-Hundred Element Random Array
(Johnson 13 April 2002[3])

13
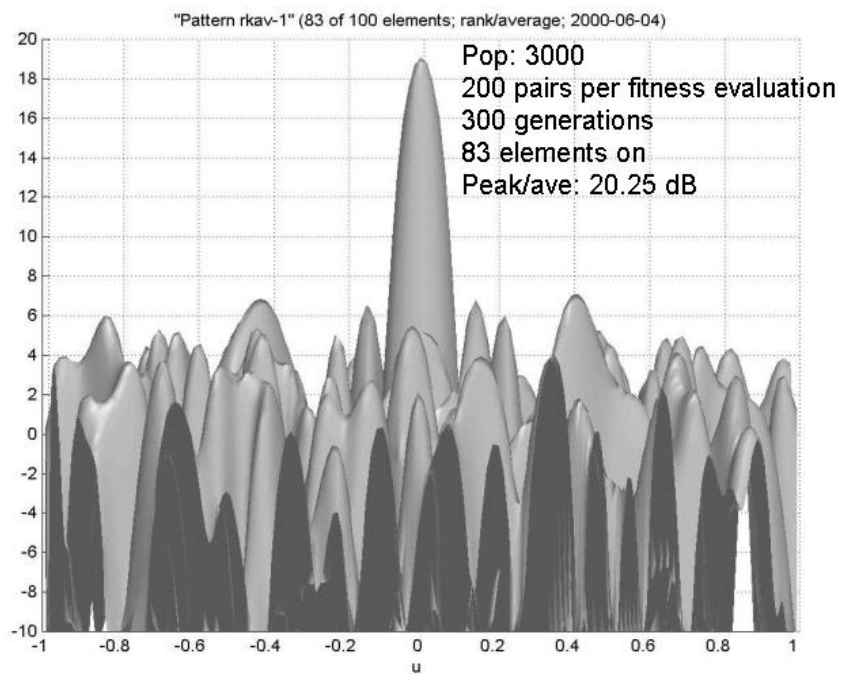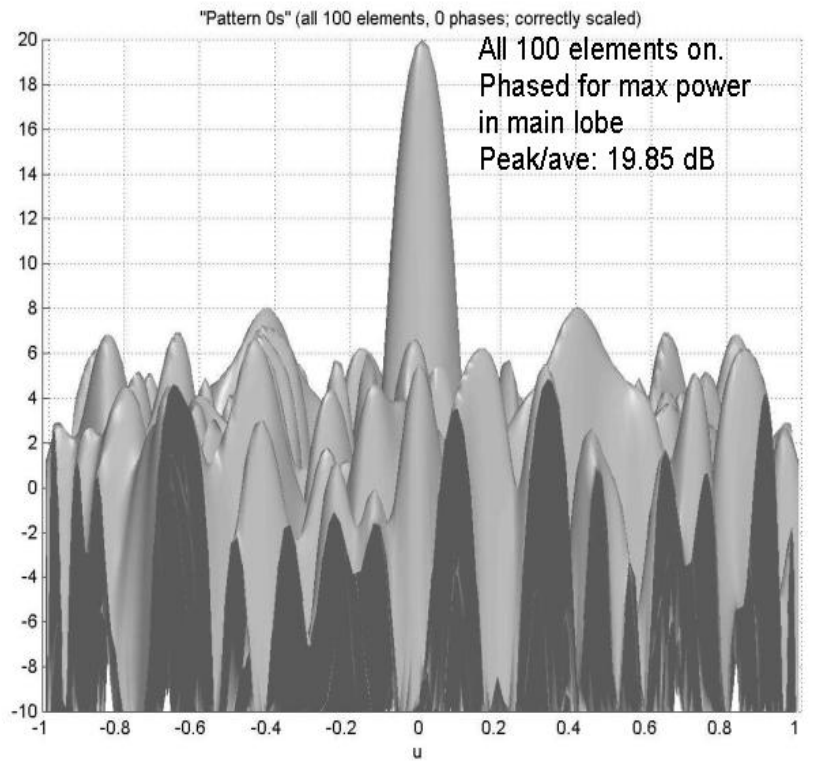
Figure 2: Conventional Solution for 100 Element Random Array
(Johnson 13 April 2002[4])

14

2.   Coordinate System

Spherical coordinates were used since they are the standard for expressing antenna patterns at a constant range. Figure 2 displays the typical polar coordinate system. Here *u, v,* and *w* are the components along the *x, y,* and *z* axes respectively of a direction vector for which an antenna pattern is to be evaluated.
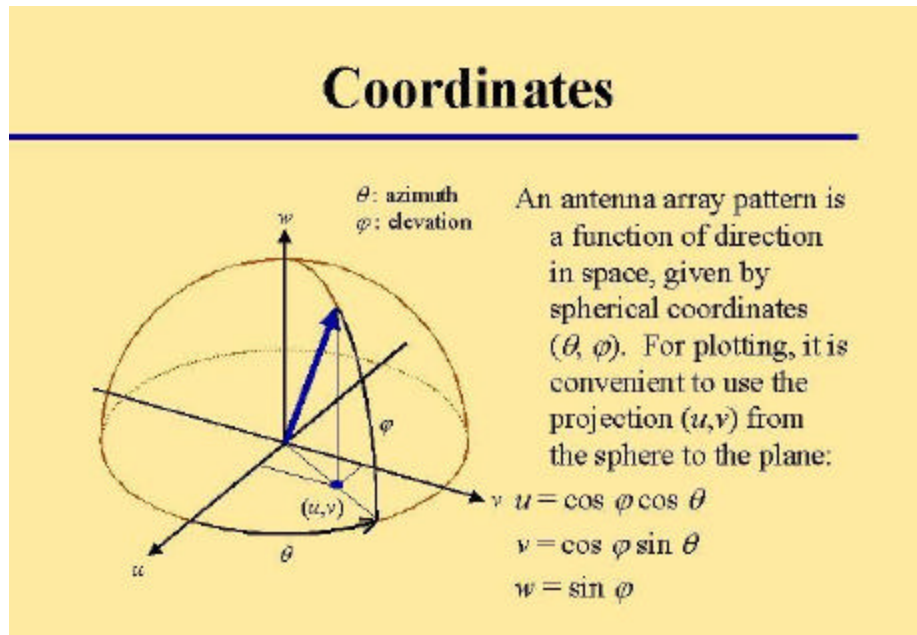
Figure 3: Coordinate System (From Johnson, 15 August 2001)

3.   Fitness Criterion

The ratio of peak main lobe power to estimated sidelobe average power is the measure of fitness for our purposes. The dimensions of the anechoic chamber at Naval Postgraduate School were used for initial EXTHIN5.m program calculations. The distance from the feed horn receiver to the antenna itself is nineteen feet. It was determined that this would be in the near field of the array based upon the following calculation:

$$R = D^2 / \boldsymbol{l}; D = 8\boldsymbol{l}$$
$$\therefore R = 64\boldsymbol{l} = 8m$$

The value of R is the range of the near field, $\boldsymbol{l}$ is the radiated wavelength, and D is aperture size in wavelengths. A near-field approximation for the main lobe focused nineteen feet was used. Average sidelobe strength was estimated by using the magnitude squared of the electric field, which is proportional to the power, over a set of random of points on the hemispherical surface in front of the antenna at a radius equal to the feed horn distance. The number of samples of the sidelobe points varied from run to run, but increases as the population evolved. Typical sample rates start in the hundreds of points and usually are several thousand by the completion of the final run. This increase of sampled points ensures there are no large hidden lobes within the result.

The EXTHIN5.m code uses a pattern builder function to compute the power at various azimuth/elevation angles. This required calculating the antenna pattern for each individual of the population. In terms of field amplitudes for a randomly distributed array, this is given by:[5]

$$G = \left(3/2m\right)R^2 \left| \sum_{k=1}^{2m} [A_k \boldsymbol{j}_k \left\{ \cos\left[(\boldsymbol{p}/2)\sin\boldsymbol{j}_k \right]/\cos\boldsymbol{j}_k \right\} e^{\left[2\boldsymbol{p}i(R-\boldsymbol{r}_k+\Phi_k)\right]}]/\boldsymbol{r}_k \right|^2$$

Where m is the number of elements in the array, in this case 24. The amplitude bit is represented by the A_k term. Without amplitude tapering, A is simply 1 if the kth element is on, and 0 if off. Define $\bar{X}_k = (X_k, Y_k, Z_k)$ where $(k = 1, ..., 2m)$, which are the

coordinates of the base locations of the elements in the ground planes. These are in units of wavelength to avoid writing $\bar{x}_k / \mathbf{l}$. Define $d\bar{x}_k = (dx_k, dy_k, dz_k)$ where $(k = 1,...,2m)$, the displacements from the ground plane locations to the dipole centers. These have a magnitude of $\mathbf{l}/4$ and are normal to the ground planes. In the geometry of the array of concern, these are given by $d\bar{x}_k = (\sin 30°, 0, \cos 30)/4$ when $X_k > 0$, $d\bar{x}_k = (-\sin 30°, 0, \cos 30)/4$ when $X_k < 0$. Let $\bar{x}_k = \bar{X}_k + d\bar{x}_k$, the locations of the dipole centers, and $\bar{x}_{k+m} = \bar{X}_k - d\bar{x}_k$, the locations of the images of the dipoles, reflected in the ground plane. Let Φ_k equal the phase of element k, $(k = 1,...,2m)$, and $\Phi_{k+m} = \Phi_k + 0.5$ $(k = 1,...,2m)$ with units of cycles not radians or degrees. The value $\bar{R}$ is the observation point (the location of the feedhorn), and $R = |\bar{R}|$ where $\hat{u}$ in the unit vector in the direction of $\bar{R}$ $(\bar{R} = R\hat{u})$. The value $\bar{r}_k = \bar{R} - \bar{x}_k$ for $(k = 1,...,2m)$ and $r_k = |\bar{r}_k|$. The $\mathbf{j}_k$ term is the complementary angle between $\bar{r}_k$ and the unit vector $\hat{j}$ in the y-axis direction $(\sin \mathbf{j}_k = \hat{j} \bullet \bar{r}_k / r_k)$. The $\hat{\mathbf{j}}_k$ term represents the corresponding polar unit vector in the plane of $\bar{r}_k$ and $\hat{j}$, and orthogonal to $\bar{r}_k$, pointing in the direction of increasing $\mathbf{j}$. (The polar coordinates $\mathbf{j}_k$ are in a system with the y-axis as the pole, and since that is the direction of the orientation of the dipoles. They are not to be confused with $\mathbf{j}$ in Figure 3, which has the z-axis as the pole.) The term in the braces, $\cos\left[(\mathbf{p}/2)\sin \mathbf{j}_k\right]/\cos \mathbf{j}_k$, is the element pattern for the half-wave dipole.

17

The resulting pattern is sampled at the chosen number of points to determine fitness. In Phase One, the value of Z for all elements was zero, i.e. the surface of the ground plane was taken to be the X-Y plane. In this phase, the geometry is three dimensional, demonstrating engineering flexibility made available by using the GA concept as a design tool.

On the actual array, the dipoles are placed over a ground plane to increase their directivity. Using images through the plane permits the representation of an apparently infinite ground plane. An image dipole is introduced for each dipole element. The currents on the image dipoles are opposite of those on the source dipoles. Thus the equivalent problem for the array over an infinite ground plane is a two-layer array in free space.[6] Note: the two ground planes at an angle complicate this simple picture. Each element's image is obtained by reflection in the associated plane.

Since no antenna element has a perfectly isotropic pattern, an element factor must be employed. The expression for G above, without the term in braces, gives the so-called "array factor", G_a. The array factor by itself was used in the original 100 element computations; however, for more accurate and realistic results, the element factor is a necessity. The element pattern for the half-wave dipole is:

$$G_e = \cos\left[(\boldsymbol{p}/2)\sin\boldsymbol{j}_k\right]/\cos\boldsymbol{j}_k$$

This term is therefore included in the pattern builder equation previously presented. Mutual element capacitive and inductive coupling and manufacturing differences between elements were assumed to be of negligible impact and ignored.

The traditional Method of Moments (MoM) calculation method accounts for these effects. These effects are small enough that the product of the array and element factors is a widely used approximation.[7]

4.   Genetic Operations

Reproduction, mutation and crossover were all used in the EXTHIN5.m code (see Appendix B, Section B3); however, inversion was not. Changing the order of each element's phase and amplitude would have an overly randomizing effect and would not be logical in supporting the desired result of optimal convergence of the beam pattern. The ratios and order of each operation were varied from run to run in an effort to promote the introduction of "random innovation" as the population members began to converge and lose diversity. The ratios are expressed in the order of a three number series (REP:CROSS:MUTATE) representing reproduction, crossover, and mutation. Rank-proportional selection method was used for all operations. Crossover and mutation operations were carried out in the same manner as "Genetic Algorithms as a Tool for Phased Array Radar Design", Master's Thesis by Jon A. Bartee, LT, USN, June 2002, as described below.

Two points were used in the crossover operation. Selecting two parents proportional to rank and two randomly chosen indices, i and j, that were in the range of 1 to N, with i always less than j were used, the values for the "on/off" bit, A_k, were swapped between these two parents for k in the range $i<k<j$, as were the phase setting, $\boldsymbol{f}_k$. Additionally, the phases at the two ends were perturbed by a

random amount proportional to the difference between the values for the two parents. The motivation for doing this was to roughly approximate the behavior that would have been obtained if the phases had been represented in fixed point binary, bit-wise two point crossover had been used, and the endpoints of the interval had fallen somewhere within the representations of the *i*th and *j*th phases.

The mutation operation was fairly straightforward. Indices *i* and *j* were chosen in the same fashion as for crossover. The elements between these two indices had their "on/off" bits replaced with a randomly selected value of either 0 or 1. Each had equal probability. Likewise, the phase values for elements between the endpoints were replaced with a new phase value, a random floating-point number between 0.0 and 1.0.

5.   Figures of Merit (FoM) and Summary of GA Runs

In order to determine the relative degree of success for the results of a series of Genetic Algorithm runs, as well as get an idea of the computational and time resources required to achieve the end results, a look at some of the more important parameters and performance characteristics of the EXTHIN5.m code is in order. Particular attention should be paid to which factors changed between runs and which did not.

The original program used for the first series of runs was EXTHIN3.m. These six runs were evolved by EXTHIN3, which used function "nfpattern4" for the pattern computations. While reviewing some of the data from the LE3 run pattern for

comparison with the MoM computations, it was determined that the radiation from the dipoles and image dipoles to the rear of the ground planes was not zero. This was not a problem in Phase One, since the pattern in the negative-z hemisphere wasn't included in the estimates of average sidelobe level However, with the ground planes tilted by 30 degrees, part of the pattern from the edges of the two sides intruded into the positive-z hemisphere and had a small effect on the computed patterns. Therefore, a new function for computing patterns, "nfpattern5", was incorporated and the new program renamed EXTHIN5.

The following points apply to all runs from both programs:

- Pentium IV 2.4 GHz computer used for all runs.
- Ground planes were folded back 30° on each side yielding a 120° wedge angle for all runs.
- Selection method was rank-proportional.
- Population size fixed at 5000.
- Fitness criteria was to maximize the main-lobe-to-average sidelobe ratio.
- Beam focused at $46.362\mathit{l}$ (approximately 19 ft), which is the feed horn distance in the anechoic test chamber.
- Constant frequency: n=2.398340GHz (l=0.125m).
- For each steering angle, four successive runs were made, with the population from the last generation of each run serving as the initial population for the next. The initial population for the first run of each set was generated randomly.

21

- The four runs for each steering angle used the following parameters:

RUN	1	2	3	4
NUMBER OF GNERATIONS	36	36	15	0
REP:CROSS:MUTATE RATIO	20:79:01	18:80:02	15:80:05	N/A
FITNESS SAMPLE SIZE	500	1000	2400	7200

- The fourth run (0 generations) did not create a new population; it simply re-estimated the fitness values for the final population with a larger number of samples. Sometimes this led the program to select a different individual from that selected at the end of run 3 as best of generation. For each individual selected as best of generation, the program prints two fitness estimates: (1) the estimate based on the number of random samples indicated in the table above, and on the basis of which the selection is made; (2) a presumably more accurate estimate based on a fixed grid of 16641 sample points. When the latter estimate indicated that the selected best individual from run 4 was better than the one from run 3, the run 4 results were accepted as the end result of the set of runs; otherwise it was discarded and the run 3 results were accepted. (The fitness difference between the two individuals was generally quite small.) Fitness values reported below represent estimate (2), based on the large fixed grid.

22

For each set of runs, the following information is presented.

- Steering direction is in polar coordinates (q, f); f is the "elevation" or altitude of the vector above the xy plane (the complement of the angle with the z-axis); q is the "azimuth" or the angle of the projection of the vector into the xy plane, measured counterclockwise from the x-axis. (See Figure 3)

- The corresponding direction cosines are u, v, and w with respect to the x, y, and z-axes.

- The corresponding y-based polar coordinates of bearing and elevation. "Elevation" is that of the vector above the zx plane (complement of the angle with the y-axis), and bearing is measured in the zx plane, counterclockwise from the z-axis. (So a positive bearing is on the positive x side, which is left if you stand at the origin and face in the direction of the z-axis.)

- Angles between the vector and the normals to the two ground planes, on the $-x$ and $+x$ sides (in that order).

- Number of runs. The value 4 indicates that the result of run 4 was accepted as the final result; a 3 indicates that it was rejected and the result from run 3 was retained.

- Fitness values for the individuals selected as best of generation at the end of each run.

- Logarithmic fitness values (in dB) directly below in the same order.

- Number of "on" elements on the $-x$ and $+x$ sides (in that order).

23

Table 1 summarizes the results for all GA run geometries examined with EXTHIN3.m while Table 2 lists the data from EXTHIN5.m runs.

PARAMETER	RUN TITLE	LE3	LE4	LE5	LE6	LE7	LE8
STEERING DIRECTION	DESIG	BROADSIDE OR BORESIGHT	ZX PLANE 45° FR -x AXIS	ZX PLANE 60° FR -x AXIS	ELV 50° ABOVE ZX PLANE 20° TOWARD +x AXIS	ELV 48° ABOVE ZX PLANE 12° TOWARD +x AXIS	ELV 30° ABOVE ZX PLANE 20° TOWARD +x AXIS
STEERING DIRECTION (Z-POLAR)	q	000	180	180	073.9871	079.3967	059.3577
	f	090	045	060	037.1586	040.8824	054.4687
DIRECTION COSINES	u	0.0	-0.7071	-0.5000	0.2198	0.1391	0.2962
	v	0.0	0.0	0.0	0.07660	0.7431	0.5000
	w	1.0	0.7071	0.8660	0.6040	0.6545	0.8138
Y-BASED POLAR COORD'S	brg	000	-045	-030	020	012	020
	elv	000	000	000	050	048	030
GROUND PLANE NORMALS	-x	030	015	000	065.5955	060.1810	56.1741
	+x	030	075	060	050.7265	050.4775	31.4749
# OF RUNS		3	4	4	4	3	4
FITNESS	RUN 1	54.3684	26.8466	38.4750	8.2967	10.7832	25.8931
	RUN 2	60.9952	28.1510	41.9305	9.4503	12.1283	30.1996
	RUN 3	62.6099	28.1772	43.1296	9.4421	12.3672	30.1131
	RUN 4	N/A	28.2121	43.2224	9.4979	N/A	30.1324
FITNESS (dB)	RUN 1	17.3535	14.2889	15.8518	9.1891	10.3275	14.1318
	RUN 2	17.8530	14.4949	16.2253	9.7545	10.8380	14.8000
	RUN 3	17.9664	14.4990	16.3478	9.7507	10.9227	14.7876
	RUN 4	N/A	14.5044	16.3571	9.7763	N/A	14.7903
NUMBER OF ELEMENTS ON	-x	11	11	11	11	11	11
	+x	13	0	13	13	13	13

Table 1.   Summary of GA Run Results EXTHIN3 and nfpattern4.

PARAMETER	RUN TITLE	LE13	LE18	LE19	LE20
STEERING DIRECTION	DESIG	BROADSIDE OR BORESIGHT	ELV 30° ABOVE ZX PLANE 20° TOWARD +x AXIS	ZX-PLANE 10° TOWARD -x AXIS.	ZX-PLANE 10° TOWARD +x AXIS.
STEERING DIRECTION (Z-POLAR)	q	000	059.3577	180	000
	f	090	054.4687	080	080
DIRECTION COSINES	u	0.0	0.2962	-0.1736	0.1736
	v	0.0	0.5000	0.0	0.0
	w	1.0	0.8138	0.9848	0.9848
Y-BASED POLAR COORD'S	brg	000	020	-010	010
	elv	000	030	000	000
GROUND PLANE NORMALS	-x	030	56.1741	020	040
	+x	030	31.4749	040	020
# OF RUNS		3	4	4	4
FITNESS	RUN 1	55.1422	26.7759	57.8788	56.4086
	RUN 2	63.2261	30.5780	59.1943	60.5341
	RUN 3	63.6248	30.7044	59.4725	62.7498
	RUN 4	N/A	30.8156	59.7020	62.9194
FITNESS (dB)	RUN 1	17.4148	14.2274	17.5495	17.5135
	RUN 2	18.0090	14.8541	17.7228	17.8200
	RUN 3	18.0363	14.8720	17.7432	17.9761
	RUN 4	N/A	14.8877	17.7599	17.9878
NUMBER OF ELEMENTS ON	-x	11	11	11	11
	+x	13	13	13	13

Table 2.   Summary of GA Run Results EXTHIN5 and nfpattern5.

THIS PAGE INTENTIONALLY LEFT BLANK

III. EXPERIMENTAL VERIFICATION OF THE GENETIC ALGORITHM AS A RADAR ANTENNA DESIGN TOOL

A. DETERMINATION OF GA CAPABILITIES AND EFFECTIVENESS

Validating the versatility of the GA as radar design tool was a challenging undertaking. Radar systems are traditionally expensive to develop, test, and evaluate. Millions of dollars are spent every year in the effort to push the envelope in radar design and performance. With only the Phase One initial work to refer too, and no physical transmit GA-designed radar hardware, an entirely new antenna system was designed, developed, built, tested, and evaluated with thorough documentation throughout the process. Whilst the basic functions of the EXTHIN5.m code were discussed and evaluated in Bartee, a more robust code would be required for Phase Two's active array.

B. MEASUREMENT GOALS AND OBJECTIVES

Phase One of the project validated the use of the GA for a two-dimensional, 7.6GHz, randomly located and sparsely populated passive receive array. For this thesis, the objective was to build an entire antenna system from commodity available hardware, while still testing the robustness and versatility of the GA. It was decided that the direction of research with regard to the radar geometry would be a three-dimensional, 2.4GHz, randomly located and sparsely populated, active transmitting antenna array. The objectives evolved to the more robust, diverse, and formidable tasks as follows:

- Construct 24 element, three-dimensional, dual ground-plane, active phase array using commercially available components.
- Use the genetic algorithm to find phase and amplitude values for the solution to the beam-forming problem.
- Demonstrate phased array steering and measure beam shape in the anechoic chamber.
- Compare measurements obtained in anechoic chamber with the genetic algorithm predictions and method of moments (MoM) calculations. Apply error analysis to any conflicts within the data, from the three methods of calculations. After applying error factors, determine if three methods correlate, validating genetic algorithm predictions.

It was from these objectives that this thesis' experimental basis with regard to the Genetic Algorithm versatility evolved.

C. RADAR COMPONENT DESIGN AND CONSTRUCTION

Frequency selection was crucial to project success given the limited resources. While a higher frequency would yield a physically smaller array, lower frequency components are more readily commercially available. Staying in the silicon semi-conductor realm was desired due to low cost and availability. With the assistance of Mr. James Alter of the Naval Research Laboratory's Radar Division, two possible phase shifter circuit cards were considered. Analog Devices, Inc. has two commercially available quadrature modulator microcircuit evaluation boards, the AD8345EVAL and AD8346EVAL. While the

lowest possible frequency was desired, there was a trade-off with regard to array size. As frequency goes down, array size and weight grows. A balance between the lowest desirable frequency and largest array geometry had to be reached. A 10x10 wavelength (l) array was desired; so a 1.0GHz frequency would have yielded a 3.0mx3.0m array geometry that would be quite bulky, unwieldy and heavy. The frequency selected was 2.4GHz, which was the best combination of a lower frequency, commodity available components, within the range for the AD8346EVAL, and yielded a 1.0mx1.0m array (wavelength of 0.125m and array size of $8lx8l$). This frequency was also well within the range of the Naval Postgraduate School's anechoic test chamber measurement capabilities, which made radar evaluation much easier since a specialized chamber was not required.

1. Verification Of AD8346EVAL Quadrature Modulator Phase Shifter Functionality

a. Product Description

The Analog Devices Inc. (ADI) AD8346 is a silicon RFIC I/Q modulator for use from 0.8GHz to 2.5GHz. Its excellent phase accuracy and amplitude balance allow high performance direct modulation to RF. The differential LO input is applied to a polyphase network phase splitter that provides accurate phase quadrature from 0.8GHz to2.5 GHz. Buffer amplifiers are inserted between two sections of the phase splitter to improve the signal-to-noise ratio. The inphase (I) and quadrature (Q) outputs of the phase splitter

drive the LO inputs of two Gilbert-cell mixers. Two
differential V-to-I converters connected to the baseband
inputs provide the baseband modulation signals for the mixers.
The outputs of the two mixers are summed together at an
amplifier that is designed to drive a 50Ω load.   This
quadrature modulator can be used as the transmit modulator in
digital systems such as PCS, DCS, GSM, CDMA, and ISM
transceivers. The baseband quadrature inputs are directly
modulated by the LO signal to produce various QPSK and QAM
formats at the RF output.   Additionally, this quadrature
modulator can be used with direct digital synthesizers in
hybrid phase-locked loops to generate signals over a wide
frequency range with millihertz resolution. The AD8346EVAL is
supplied in a 16-lead TSSOP package, measuring 6.5×5.1×1.1 mm.
It is specified to operate over a –40°C to +85°C temperature
range and 2.7 VDC to 5.5 VDC supply voltage range. The device
is fabricated on Analog Devices' high performance 25 micron
bipolar silicon process.[1]   Figure 4 is the electrical
schematic of the AD8346EVAL microcircuit.
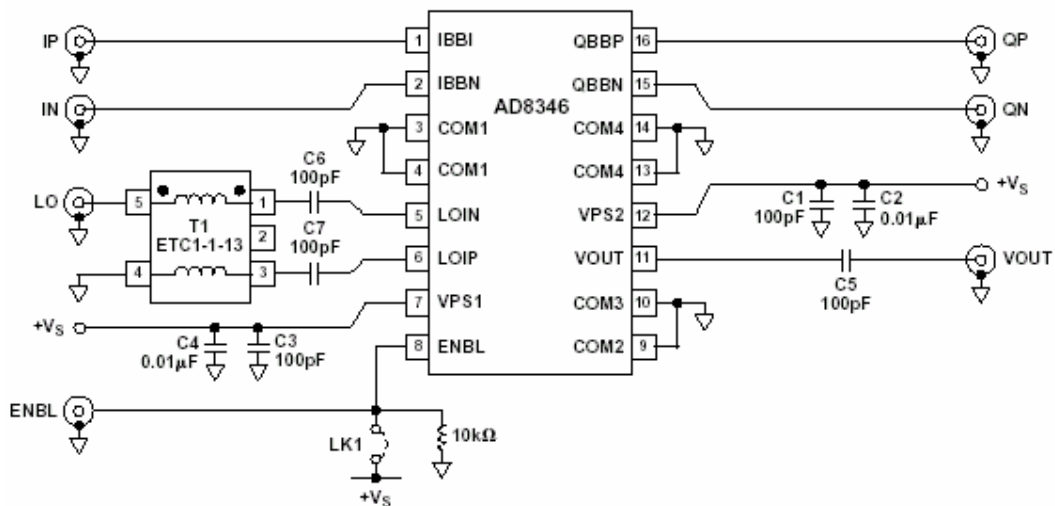
Figure 4: AD8346EVAL Circuit Diagram[2]

b. Application

The intent of the project was to use commercially
available solid-state components for phase shift, and later
amplitude tapering, in the phased array radar. Since the
frequency selected was 2.4 GHz, the AD8346EVAL board was
selected for bench test to determine if this readily available
microchip could serve as a phase shifter. Initial bench tests
were conducted to measure phase shift capability and accuracy.
According to ADI engineers, this circuit card would allow for
ninety-degree phase shifts, or phase shifts in quadrature;
however, with the assistance of Mr. James Alter, a test plan
was developed to determine if precise phase control at
arbitrary angles could be achieved.

The AD8346EVAL circuit card assembly (CCA) will only
work with positive DC voltages for phase control in this
application. There are four input pins: in-phase negative
(IN), in-phase positive (IP), quadrature positive (QP), and
quadrature negative (QN). To shift phase when a negative
value of I or Q was needed, positive voltage was applied to
the negative input pin. The phase shift quadrant determines
which two pins receive control voltage signals, while the
other two are set to zero or ground. Figure 5 displays the
typical complex phasor plane.
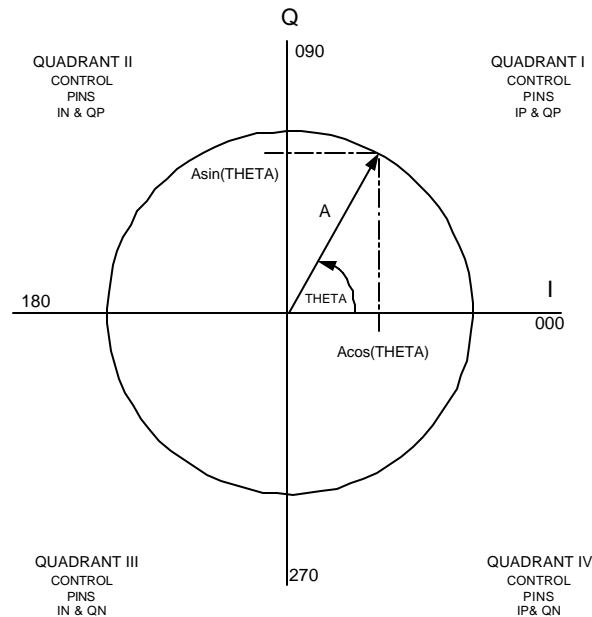
Figure 5: Complex (Phasor) Plane

Using a HP 6236B Triple Output Power Supply, a 5.000 VDC signal was applied to power the card, while 1.000 VDC was routed through a E&L Instruments Model 315-1202 Proto-Board, then through four helipots for precise control of the four input signal voltages: IN, IP, QP, QN. Amplitude of 1.0 VDC was selected making control voltages simply the cosine and sine of the phase shift angle desired. Four HP 3478A Multimeters were used to set and monitor control signal voltages. Voltage accuracy of +/- 5mVDC was possible with this bench test set up. The Vector Network Analyzer (VNA) supplied the local oscillator source signal and was able to measure the phase shift in the signal as the control signal voltages were adjusted. The VNA provided the local oscillator signal and measurement of the phase shift of that signal by the AD8346EVAL quadrature modulator. Figure 6 displays the bench test configuration while Figure 7 shows the AD8346EVAL cable connections.

32
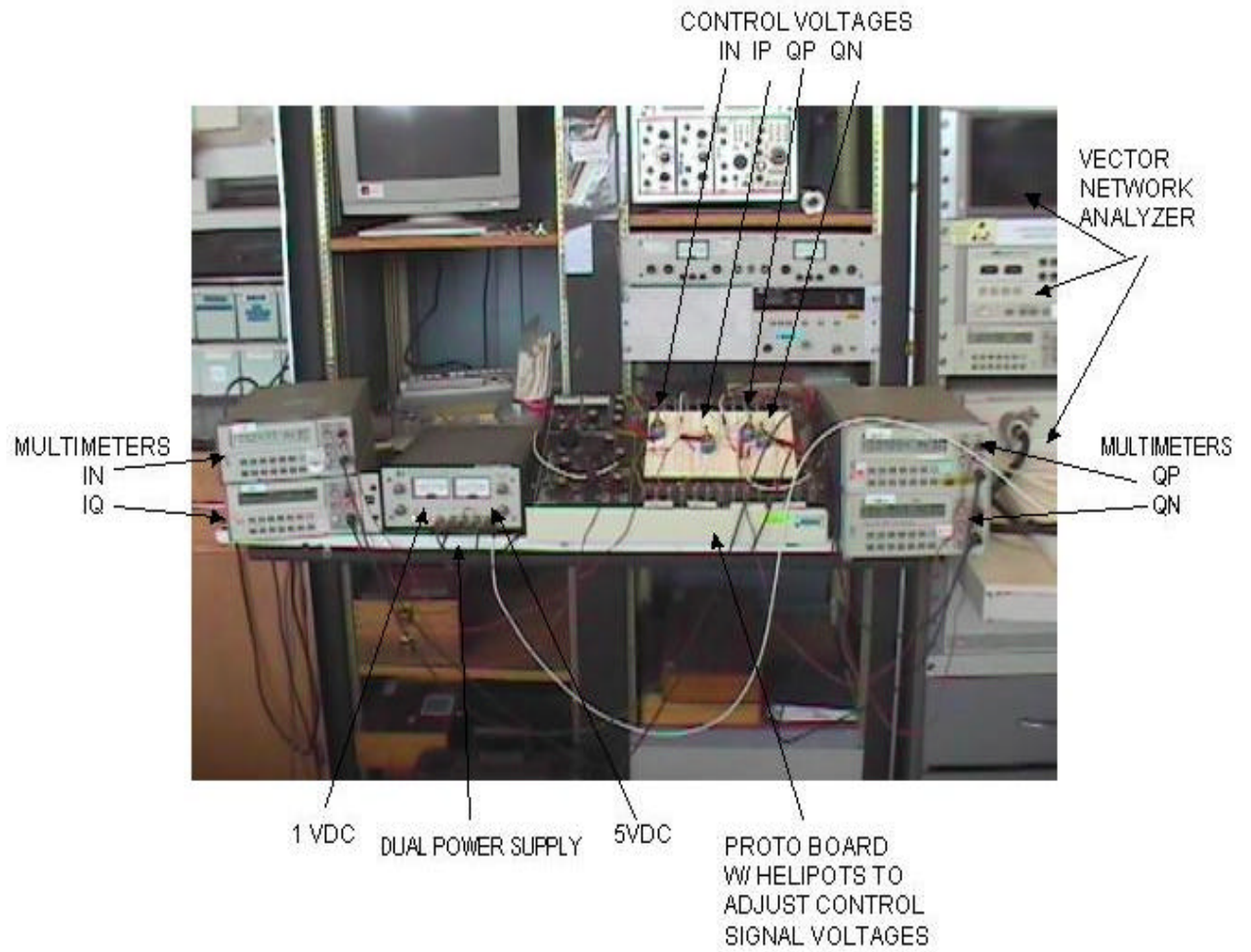
Figure 6: AD8346EVAL Bench Test Configuration
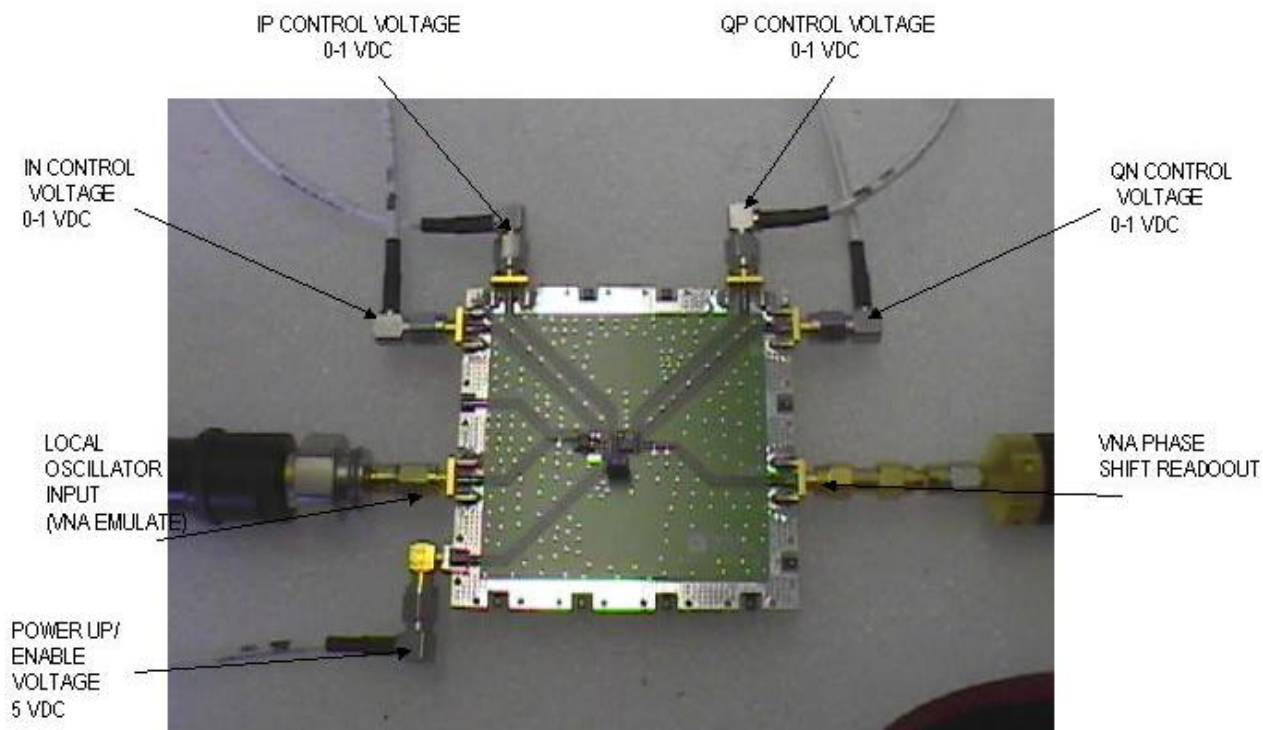
Figure 7: AD8346EVAL Cable/Signal Connections

The card PWUP (power up) input was provided with 5.0 VDC from a separate power supply. PWUP voltage above 2.0 VDC enables the card and routes the power to the VSP1 and VSP2 pins for microcircuit power. The VNA was configured to provide continuous 2.4 GHz input signal at $000.0°$ phase shift. Proper VNA calibration was completed in accordance with the HP 8510C Operator's Manual prior to connection to AD8346EVAL quadrature modulator. To shift phase in quadrant one (I+, Q+), voltages were applied to the IP and QP pins, while IN and QN are set to zero or ground. For quadrant three (I-, Q-),

voltages are applied to IN and QN respectively with IP and QP grounded or zero voltage.

SIGNAL ⟍ PHASE SHIFT	IN	IP	QP	QN
000–090	0	cos$q$	sin$q$	0
090–180	cos$q$	0	sin$q$	0
180–270	cos$q$	0	0	sin$q$
270–360	0	cos$q$	0	sin$q$

Table 3.   Control Signal Value Selection and Routing

The test bench was configured for a $360°$ sweep in $15°$ increments. The VNA was calibrated in "response mode", with the AD8346EVAL powered up, and VNA connected to the LOIN and VOUT with IP set to 1.000 VDC. When calibration was complete, the phase was $000.0°$, as desired. Measurements were made in $15°$ increments with voltage accuracy to within 1mVDC. Error in phase was observed to be greatest in the $30°-60°$ portions of each sector. Measured error was less than $1.0°$ on the I and Q axes $(000°, 090°, 180°, 270°)$. It was also noted that error was positive in lead phase angles, and negative in lag phase angles. For example, in shifting $+45°$ phase (IP=0.7071 VDC and QP=0.7071 VDC), the actual value measured was $49.3°$; whereas a $-45°$ phase shift (IN=0.7071 VDC and QN=0.7071 VDC) yielded a measurement of $-39.8°$. Power loss through was approximately -15dB, as measured with an HP E4419B EPM Series Power Meter. This value is within the range specified within the AD8346EVAL data sheet. Table 2 lists the results of AD8346 Phase Shift Bench Test.

Desired Phase	IP(mVDC) Voltage	IN(mVDC) Voltage	QP(mVDC) Voltage	QN(mVDC) Voltage	Measured Phase (Φ)	Error
0	1000	0	0	0	0	0
15	965.9	0	258.8	0	18.1	3.1
30	866	0	500	0	34.6	4.6
45	707.1	0	707.1	0	49.3	4.3
60	500	0	866	0	62.7	2.7
75	258.8	0	965.9	0	75.2	0.2
90	0	0	1000	0	89.2	0.8
105	0	258.8	965.9	0	107.5	2.5
120	0	500	866	0	124.8	4.8
135	0	707.1	707.1	0	140.2	5.2
150	0	866	500	0	153.9	3.9
165	0	965.9	258.8	0	166.7	1.7
180	0	1000	0	0	–178.8	1.2
195	0	965.9	0	258.8	–160.5	4.5
210	0	866	0	500	–144.3	5.7
225	0	707.1	0	707.1	–129.8	5.2
240	0	500	0	866	–116.8	3.2
255	0	258.8	0	965.9	–104.4	0.6
270	0	0	0	1000	–90.6	0.6
285	258.8	0	0	965.9	–72.2	2.8
300	500	0	0	866	–55.1	4.9
315	707.1	0	0	707.1	–39.8	5.2
330	866	0	0	500	–26.3	3.7
345	965.9	0	0	258.8	–13.8	1.2
360	1000	0	0	0	–0.1	0.1

Table 4.   Results of AD8346 Phase Shift Bench Test

To verify phase accuracy among all of the individual AD8346EVAL CCA's, the card for element #1 was tested in 30° increments. Phase error with the same IP of 1.000VDC was 22.3° from that of the demo test card. Due to the inherent phase error associated with path length difference, each individual elements path length would have to be measured using the VNA. These variances in path length, thus phase, would be

36

accommodated for in the initial settings of the National Instruments (NI) PXI system and offsets provided.

Possible sources of error include:

1) SMA connections, if not properly fastened can result in phase error of approximately $3°$. Wavelength at 2.4GHz is 0.125m or 125mm. Dividing $360°$ by 125mm results in a phase error of $2.88°$ per 1.0 mm of length. This equates to approximately one full turn of an SMA connector.

2) Voltage settings via DC power supply through helipot allowed only for less than 0.001 VDC resolution, or 1mVDC. For example, in setting the DC input to 200 mVDC, the meter might read 200, but the actual value could be 199.5 – 200.4 mVDC due to rounding error.

3) Values of DC voltage correspond to the sine and cosine of the phase angle respectively. For phase shift of 15 degrees, IP is set to 966 mVDC and QP to 259 mVDC. The actual values required are 965.9258•••VDC and 258.8190•••mVDC respectively.

When the National Instruments DAC's were available for installation, full accuracy was achieved; however, ADI quotes " one degree of phase accuracy at 1.9 GHz in quadrature". This was the limiting factor and overshadowed any quantization error from the 16-bit DAC's.

2.   Component Configuration

The heart of the array's control lies in the embedded processor located in the National Instruments (NI) PXI-1042 chassis. NI selected this particular chassis to provide for an embedded processor and six Digital-to-Analog Converters (DAC's). The embedded processor is an Intel Celeron 566 MHz processor running Windows NT2000 for the operating system. There are ports for monitor, keyboard, mouse, printer, and ethernet devices. Of particular note, is the capability of the entire system to be run via remote control from a notebook computer via TCP/IP ethernet connectivity. Figure 8 illustrates the NI PXI-1042 chassis.
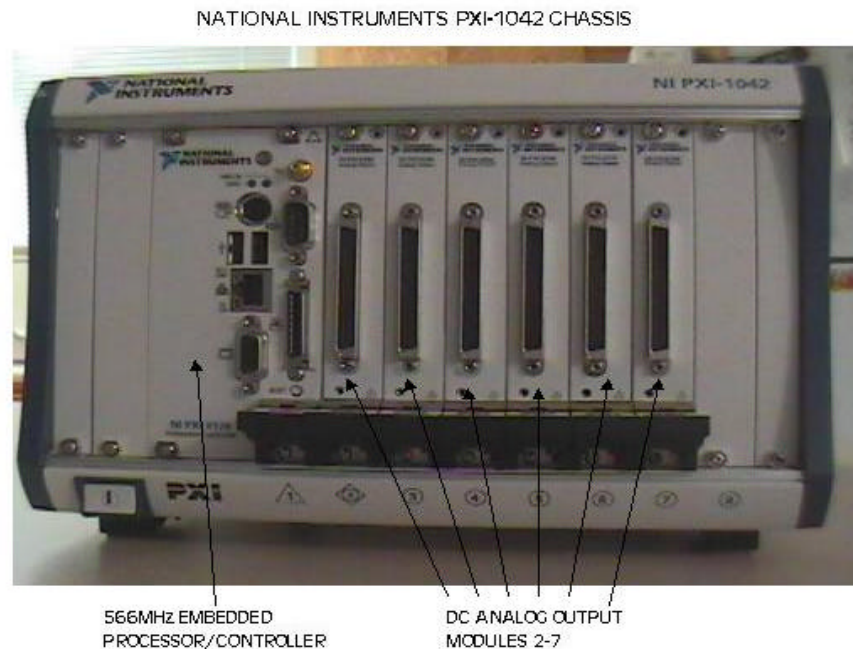
Figure 8: National Instruments PXI-1042 Chassis

LabVIEW version 6.1 was used to generate the actual control program that sets the amplitude and phase of each individual element. The program "ConversionFinal.vi" imports amplitude and phase data from the Genetic Algorithm (GA) calculations completed via MATLAB. The amplitude (A) and phase $(\boldsymbol{q})$ data is converted in LabVIEW to in-phase (I) and quadrature (Q) settings. A calibration offset, $(\boldsymbol{f})$ is applied to $\boldsymbol{q}$ to account for phase errors associated with path length differences from local oscillator (LO) signal output to each individual radiating dipole element. ConversionFinal.vi then calculates the required control voltage for the desired phase shift according to the following equations:

$$I = A\cos(\boldsymbol{q} - \boldsymbol{f})$$
$$Q = A\sin(\boldsymbol{q} - \boldsymbol{f})$$

The program sends the required control voltage signals to the required control points. As previously discussed in the application of the Analog Devices Inc. (ADI) AD8346EVAL Quadrature Modulator circuit card assembly (CCA) as a phase shifter, the NI PXI-6704 DAC's send control voltages signals to the respective inputs, IN or IP, QP, or QN via SRC-316 low voltage, low frequency coaxial signal cable. The capability of using strictly DC voltages for the control signals is what allows the AD8346EVAL quadrature modulator to be used as a dedicated phase shifter.

Each ADI AD8346EVAL CCA has four SRC-316 signal cables attached; one for each control signal voltage. These cables are attached to the NI TBX-68 terminal block with is connected by an NI SH-6868-D1 cable to each DAC. Each NI PXI-6704 DAC controls four AD8346EVAL CCA's. Terminal block routing configuration is illustrated in Figure 9.
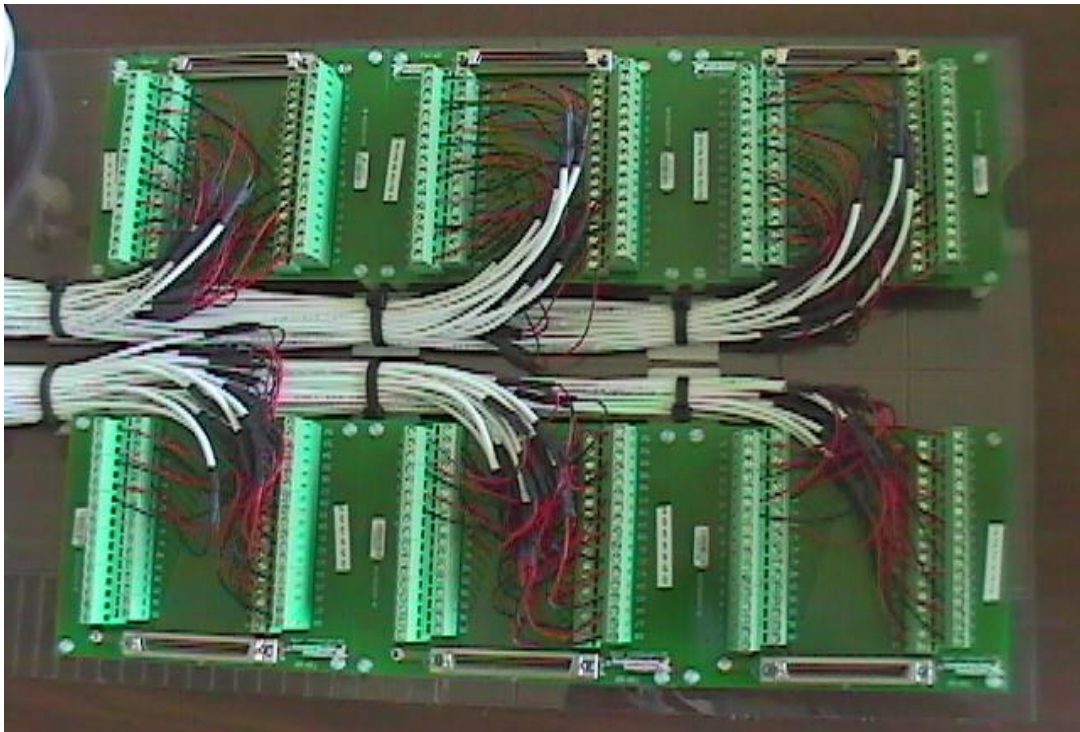
Figure 9: National Instruments TBX-68 Terminal Blocks with
SRC-316 Control Signal Cables connected

40

The 5.0 VDC power up signal is provided by a Total Power International brand T-40C triple DC power supply. This power supply provides 5.0 VDC via SRC-316 coaxial cables for the 24 AD8346EVAL CCA's, and the power up and tuning voltage for the Z-Communications V800ME10 2.4GHz LO signal. The turning voltage is routed through a 1kO helipot for fine-tuning of the LO frequency. LO construction is shown in Figure 10.
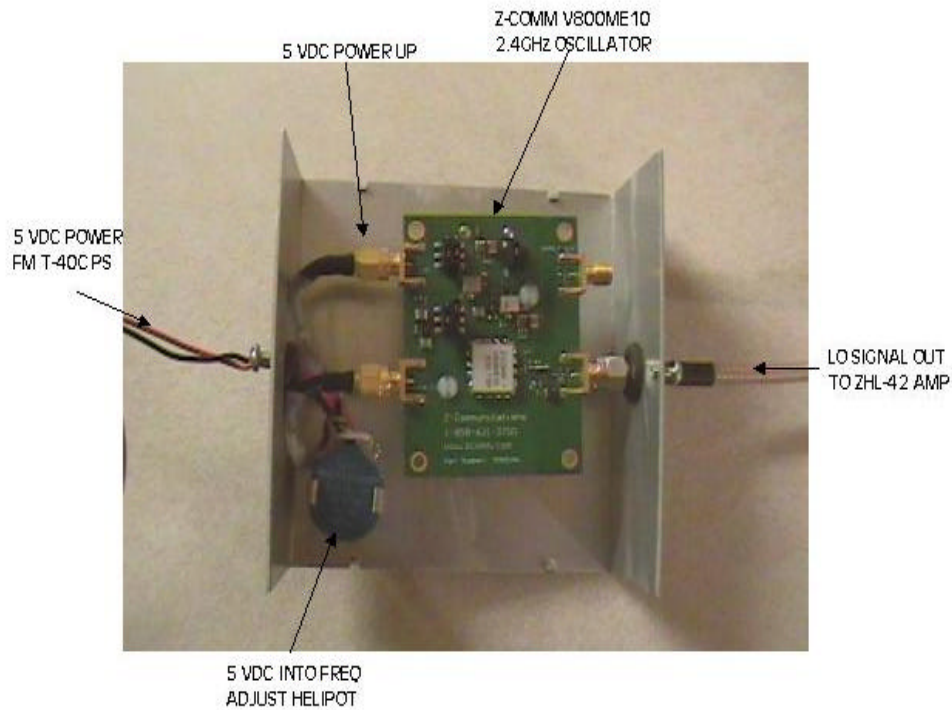
Figure 10: LO Construction, Internal Configuration

The 24 AD8346EVAL CCA's are mounted in two fabricated racks; each holding twelve CCA's each. AD8346EVAL mounting racks are shown in Figure 11.
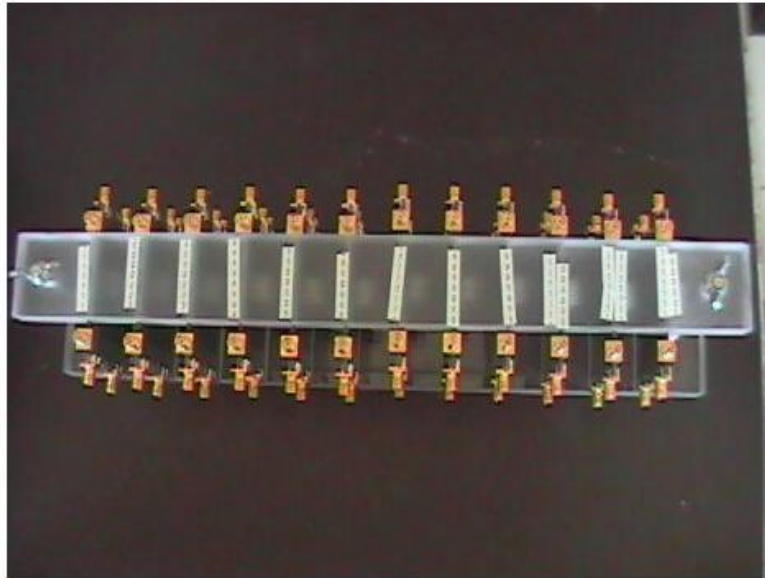
Figure 11: AD8346EVAL Fabricated Mounting Rack

The 2.4GHz LO signal that is generated by the Z-Communications V800ME10 Oscillator, is then passed through a Mini-Circuits ZHL-42 amplifier. The 15 VDC power is provided by the same T-40C DC power supply that provides the 5.0 VDC to the LO and the 24 AD8346EVAL CCA's. A switch box allows for the amplifier to be powered up before the LO in accordance with the amplifier manufacturer specifications. This signal is then attenuated 6.0 dBm and passed through a Meca Electronics 4-way power divider, then each of the four outputs is then passed through a Meca Electronics 6-way power divider

42

to provide for 24 individual 2.4GHz LO inputs to each
AD8346EVAL CCA. Since maximum input power to the AD8346EVAL
is +10dBm, but the ZHL-42 amplifier boosts the LO signal to
+36dBm, with a 14dBm loss from the power dividers, the in-line
attenuator is used to further reduce the signal strength to
the maximum +10dBm. The local oscillator circuit is shown in
Figure 12.
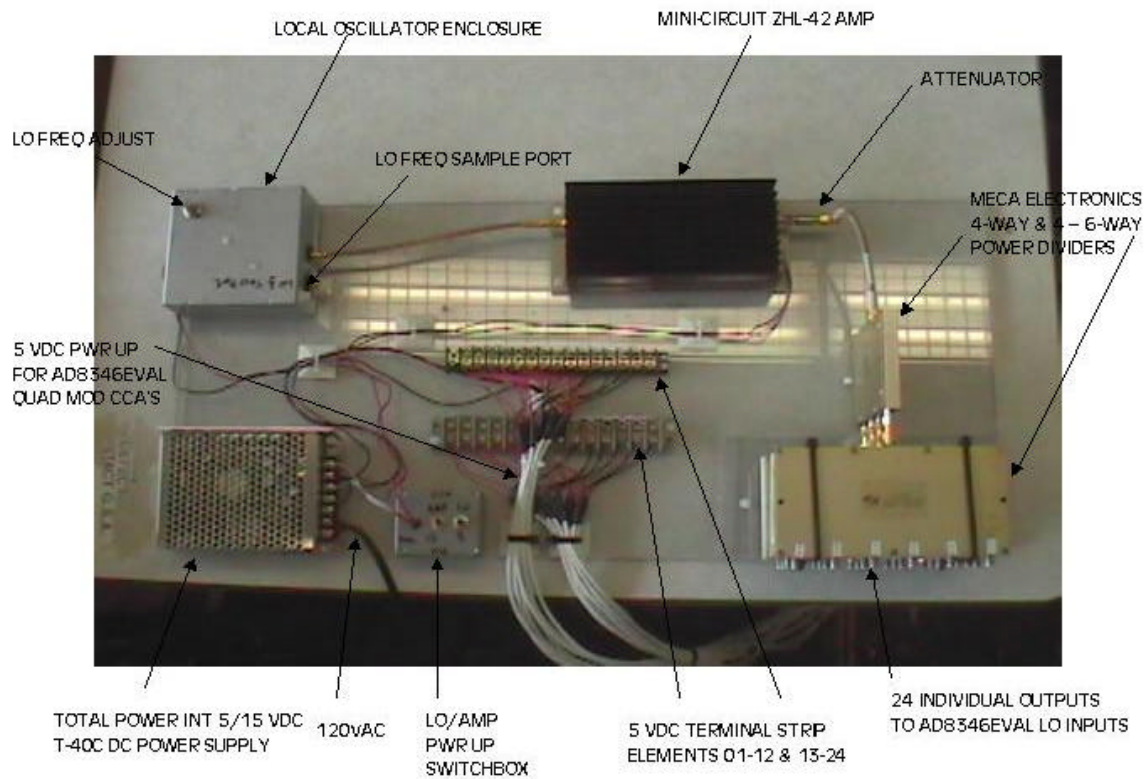
Figure 12: Local Oscillator Routing Panel

Local oscillator signal routing is achieved through the
use of SRC-402SF T-FLEX flexible microwave cable. T-FLEX
cables allow for increased flexibility in signal path routing,
without inherent limitations of the rigid 0.141" wave guide

43

material.   T-FLEX cables are path length matched from SRC to be within $+/-2.5^{\circ}$.

The output signal from each AD8346EVAL "phase shifter" is then routed its corresponding dipole element with an SRC-402SF T-FLEX cable.   The dipole elements were specified as 50O impedances for proper impedance matching with the AD8346EAVAL CCA's.   Appendix C lists the complete component inventory. The completed radar equipment cart is displayed in Figures 13 and 14 below.
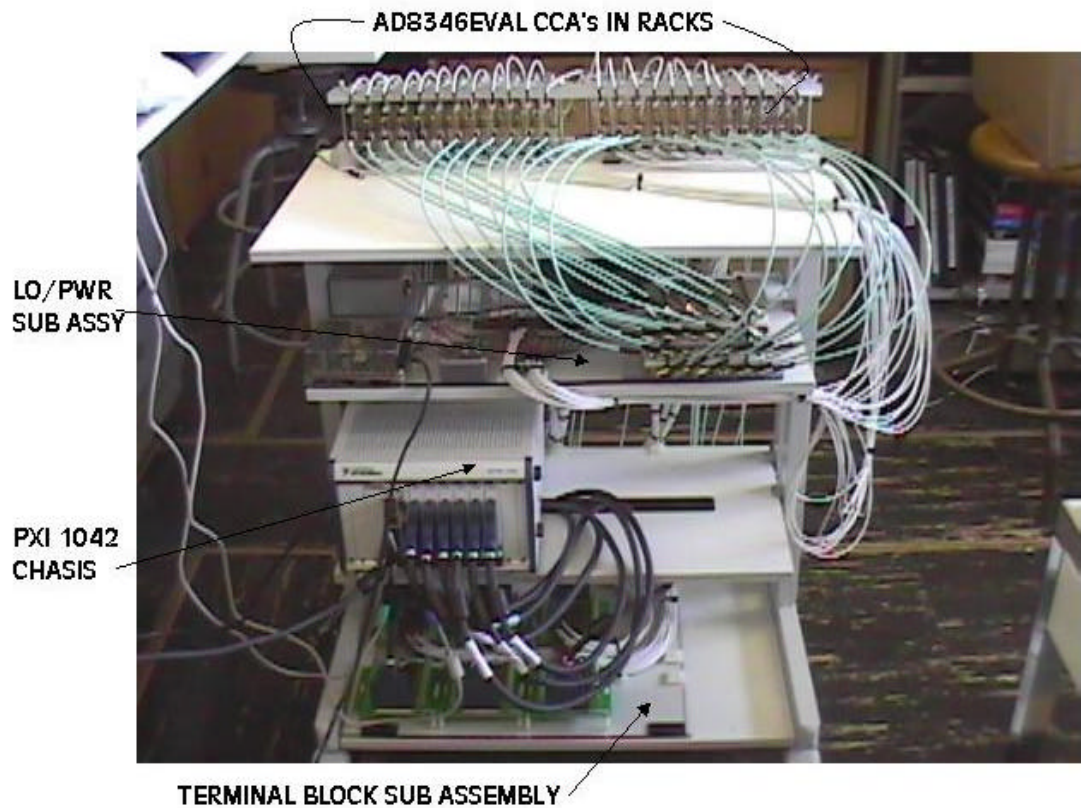
Figure 13: Equipment Cart Front View
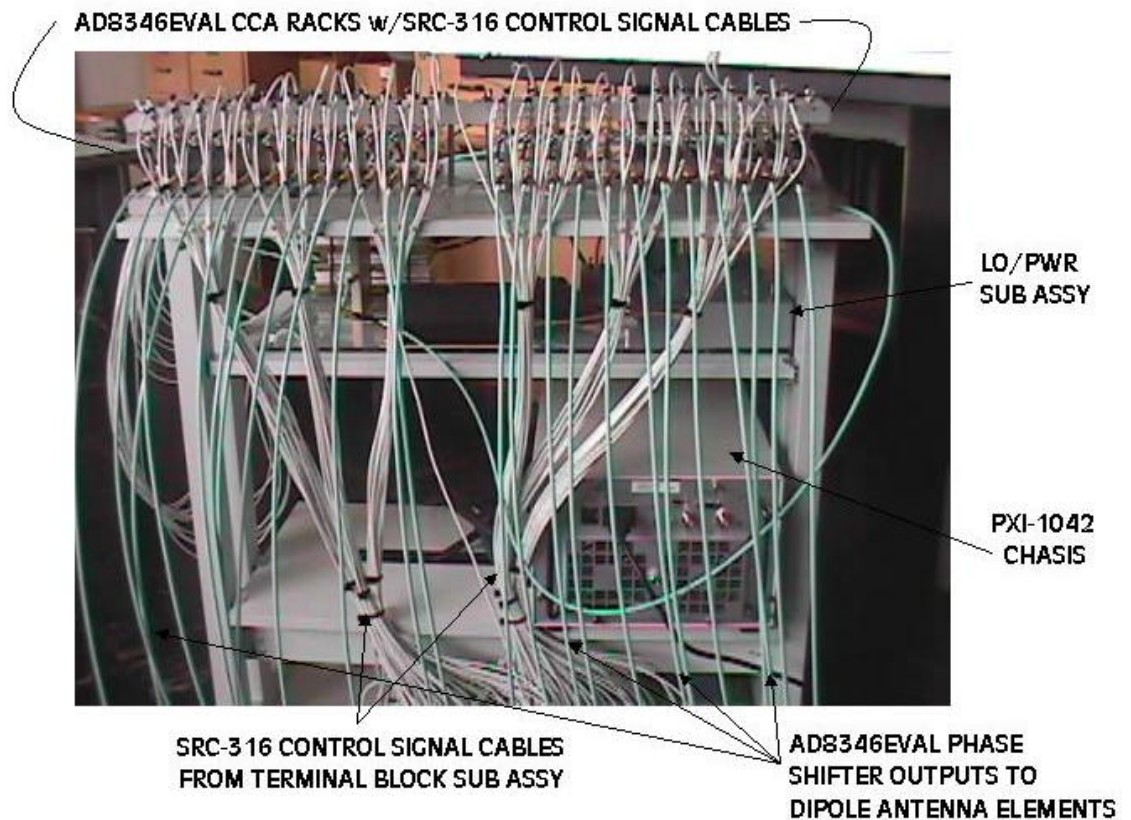
Figure 14: Equipment Cart Rear View

3.   Physical Array Construction

The physical antenna array dual ground planes were each fabricated from 7075T6AL 3/16" aluminum plate. Each ground plane measures 1.0m tall x 0.5m wide $(8\textit{l}\, x 4\textit{l})$. The two plates were then connected together by an ABS plastic piano hinge providing isolation between the two planes. The array base was fabricated out of 1" thick polycarbonate plastic plate. This base was later changed to ½" thick plywood to limit the reflection from the base. The array is hinged allowing for three-dimensional geometry variations from $000-045°$ per side. The included angle between the two ground planes can be

45

adjusted from 090−180°. Figure 15 shows the basic array layout
and XYZ coordinate axes.

GROUNDPLANE   INCLUDED ANGLE   GROUNDPLANE
                     ADJUSTABLE 090-180

TOP VIEW

FOLDBACK ANGLE   FOLDBACK ANGLE
ADJUSTABLE 0-45   ADJUSTABLE 0-45

+x AXIS

+z AXIS

FRONT VIEW   SIDE VIEW

+y AXIS   +y AXIS

+x AXIS

+z AXIS
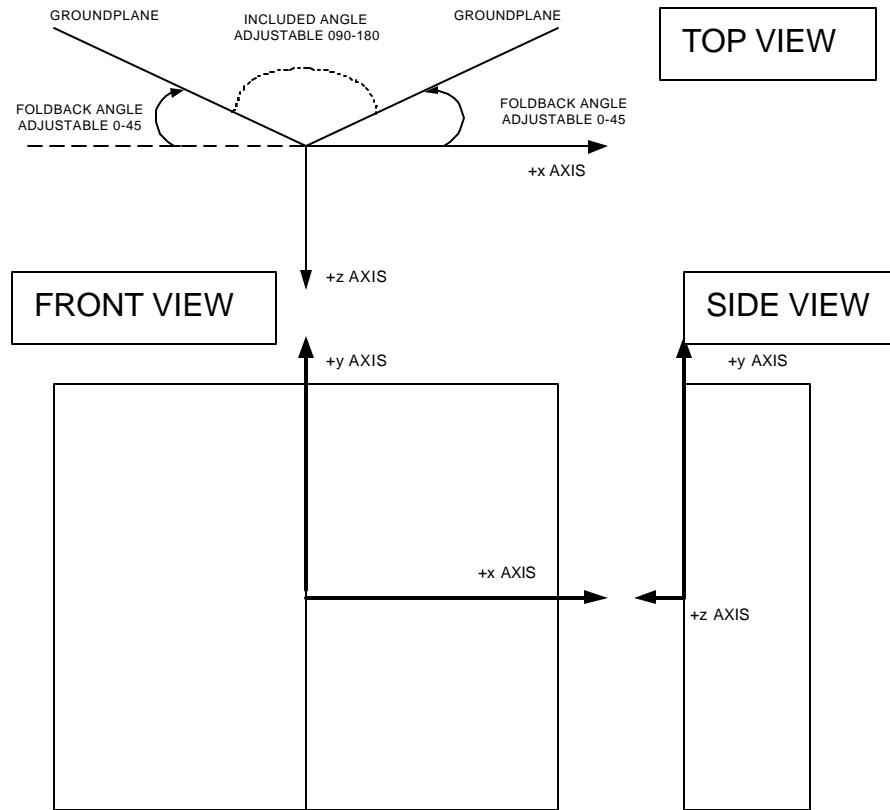
Figure 15: Array Ground Plane Geometry

Element locations were randomly generated with the constraint
that minimum spacing was $l/4$ on x-axis and $l/2$ on the y-axis
between elements. These locations are listed in Appendix D.
Figures 16 and 17 show the front and back of the antenna.
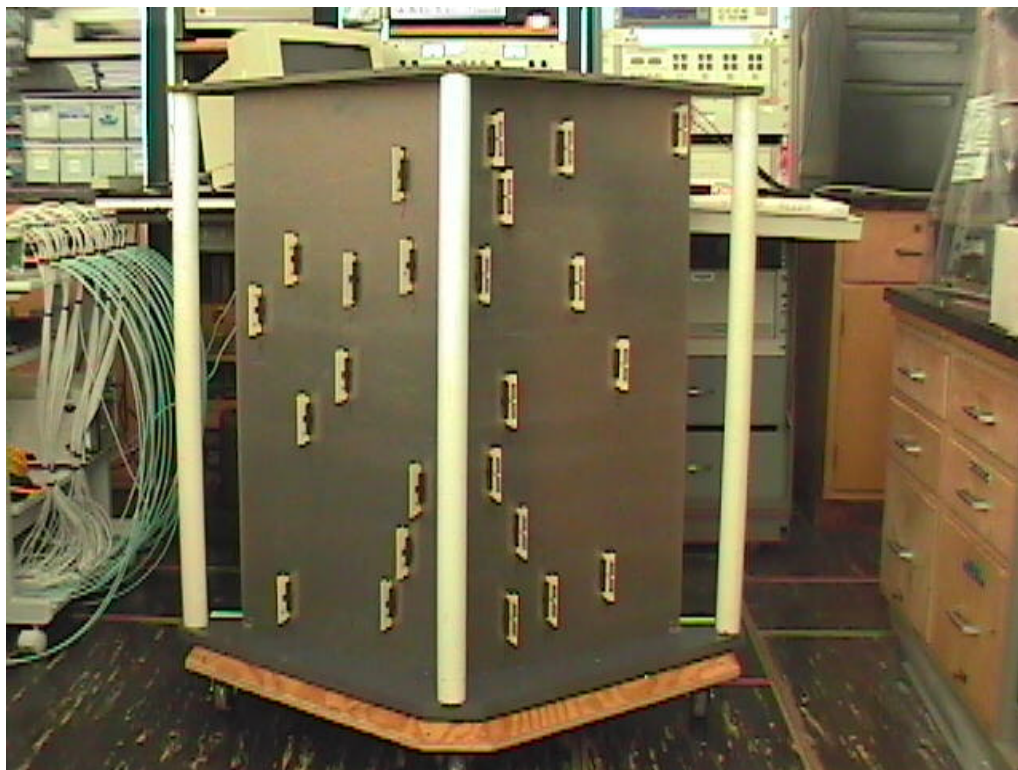
Figure 16: Antenna Front View
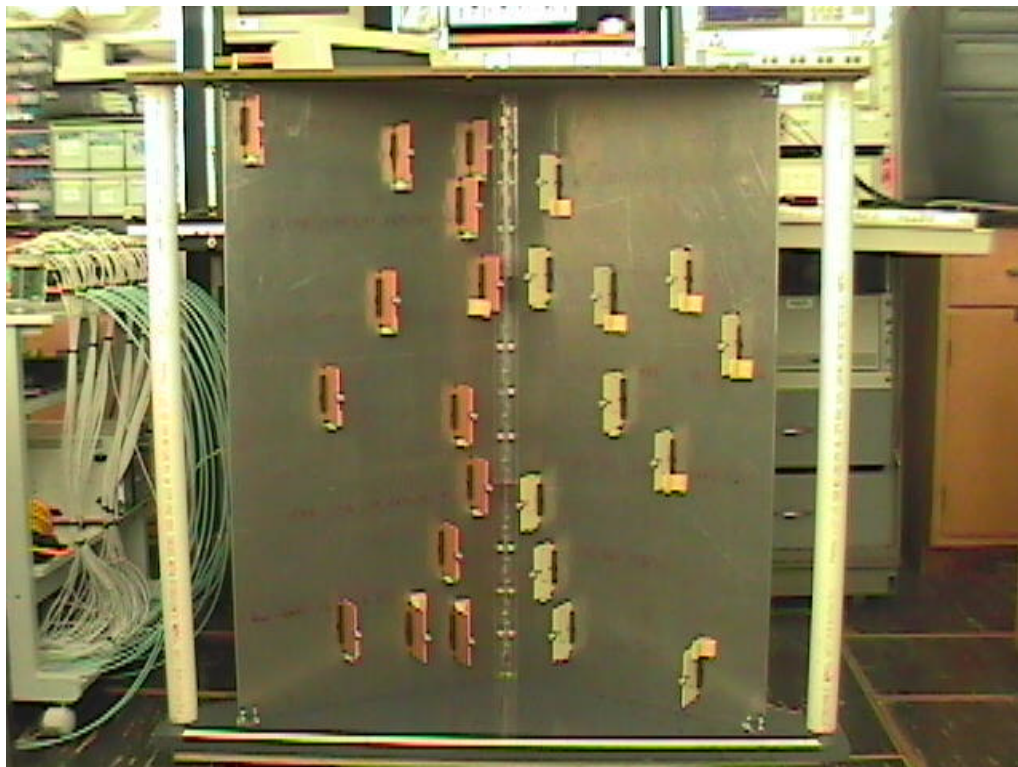
Figure 17: Antenna Rear View

47

One of the challenges in the array construction was the mounting of the dipole elements. Each dipole had a small rubber U-groove strip placed top and bottom where it passed through the array and made contact with the metal plate. The dipole was held in place with rubber weather-strip and positioned with l/4 length extended above the ground plane. Small 1"x1" L-shaped wood clips were used to ensure the dipoles remain perpendicular to the array plane. Double-sided foam tape was used to secure the elements and clips to the ground plane.

Return loss measurements were conducted with the VNA to ensure that the radiating dipole elements were adequately electrically isolated. Return loss as measured with the VNA was borderline at −15dB. The cause of this was that the slots were too narrow. Reflectivity increased because of impedance mismatch due to the shorting of the electric field of the dipole element in free space. A routing bit was used to make a ¾" hole in the center of each slot so that the standoff distance was increased between the ground plane and the feed lines of the dipoles as they passed through the array surface. By increasing the standoff distance, the field disruption was reduced, allowing for proper impedance matching. The return loss improved to the range of −18dB to −23dB as measured with the VNA. Figures 18 and 19 display the mounting detail of the elements.
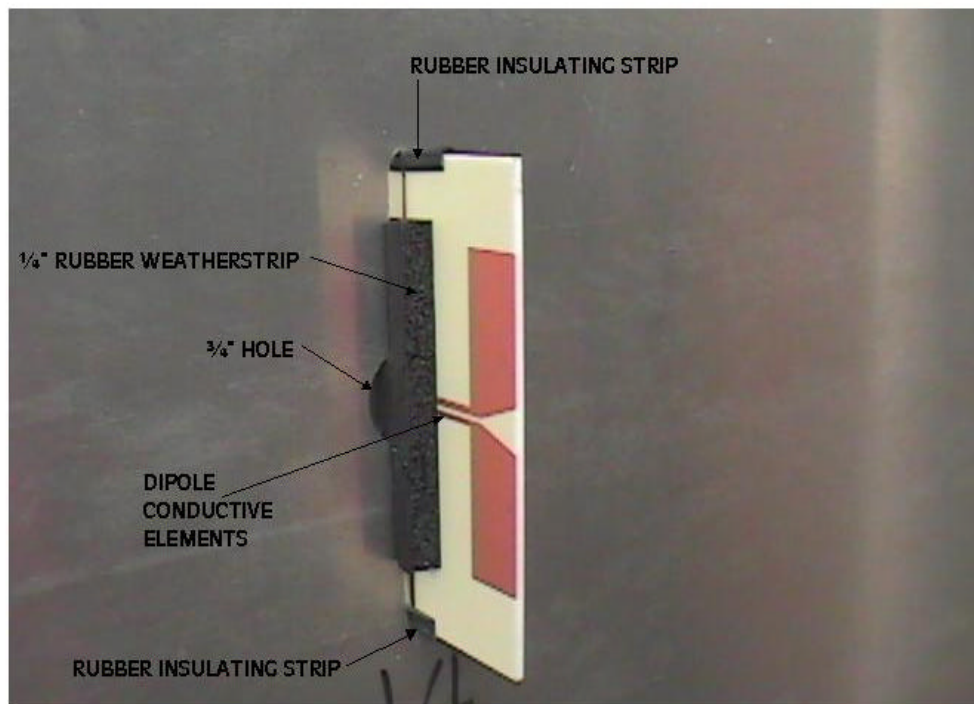
Figure 18: Dipole Element Mounting, Front View
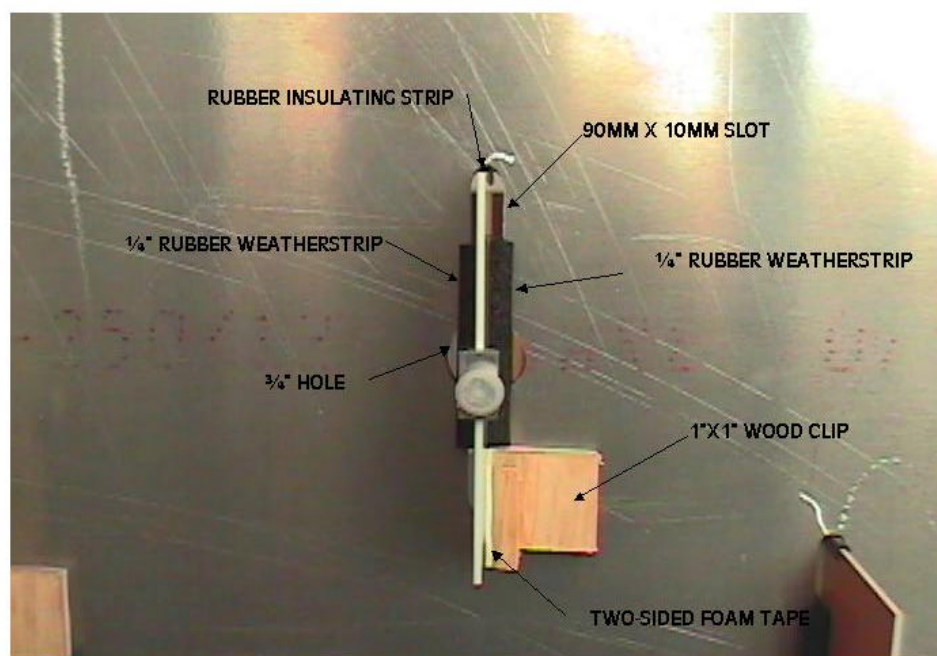
Figure 19: Dipole Element Mounting, Rear View

4. System Block Diagram

Overall system configuration is shown in Figure 20. Appendix E contains schematics for the major sub-systems.
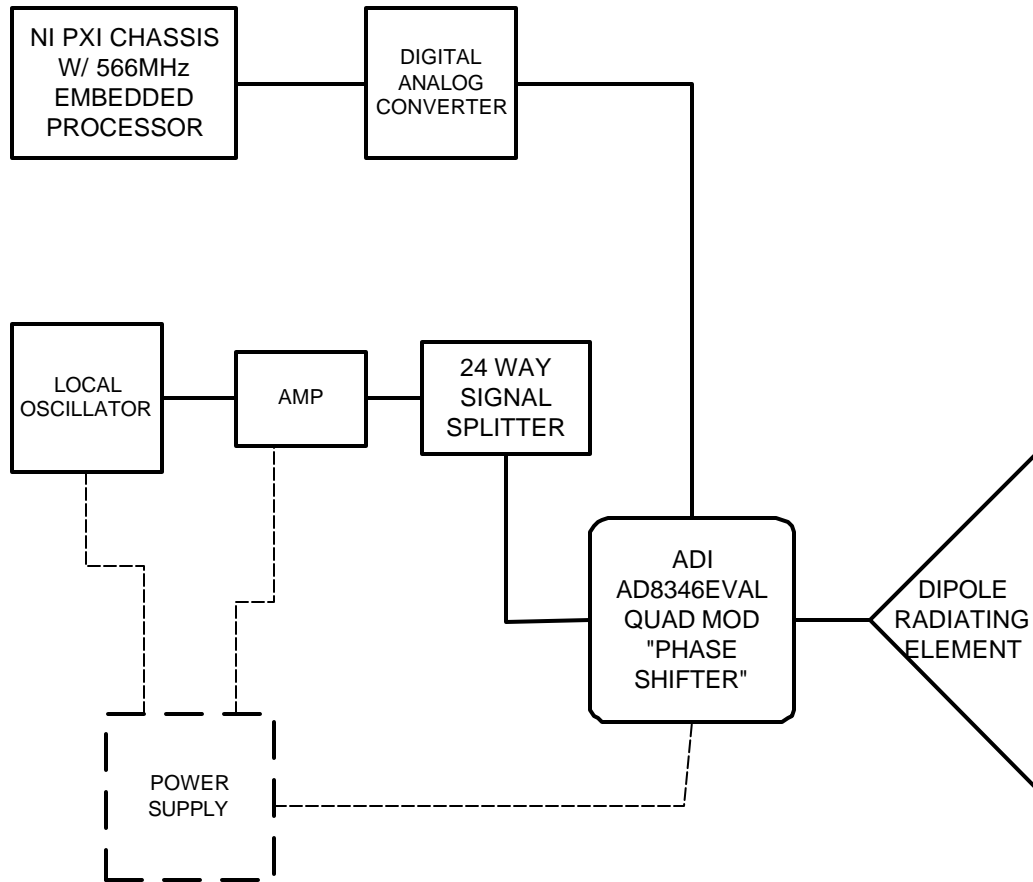
Figure 20: Master Configuration Diagram

D. LABORATORY INSTRUMENTATION AND TEST EQUIPMENT

All laboratory tests and measurements were conducted using the HP 8510C Vector Network Analyzer (VNA). The primary subcomponents of the VNA are the HP 85101 Display and Processor, the HP 85102 IF detector, the HP 8517A two-port S-Parameter Test Set, and the HP 83651A Synthesizer-Sweep

Generator. These components comprise a complete test system that provides a stimulus to the device being tested and measures the response of the device. The system allows the operator to select from various data displays including power and phase displays. Calibration techniques and procedures permit measurement at the interface of the device under test, minimizing the effect of systematic measurement errors. The HP E4419B EPM Series Power Meter was used for all power measurements.

E.   CALIBRATION AND TEST PLAN

Before all subassemblies were connected together and configured as an entire unit, certain tests and calibrations were conducted to verify accuracy and integrity of the systems individually and as a whole unit.

1.   Control Cable Pin-Out Signal Verification

Using the embedded processor in the PXI-1042 chassis running the LabVIEW control program, voltages were applied to each output pin and SRC-316 control signal cable that connects to each AD8346EVAL element. The cables provide the pathway for the IN, IP, QP, and QN signals to the AD8346EVAL CCA. Each cable is interfaced with a NI TBX-68 terminal block. By applying a $45°$ phase shift to every element (IP=0.7071 VDC, QP=0.7071 VDC) all IP and QP pin connections were verified correct. Then by applying a $-135°$ phase shift (IN=0.7071 VDC, QN=0.7071 VDC) all IN and QN pin connections were checked. All pin-outs were verified using a Tektronix DMM916 Multimeter to measure the proper voltage was applied and insure that all

pins and signal cables were connected correctly. Appendix F lists the pin-outs and signal connections.

2. Local Oscillator Signal Path Integrity

Verification of the LO signal pathway had to be confirmed. By measuring the power out of each component in the path, verification of proper LO signal input to each AD8346EVAL element was conducted using the HP E4419B EPM Series Power Meter. Since the AD8346EVAL maximum LO input power is +10dBm, it was imperative to ensure that value was not exceeded to prevent CCA damage. LO power out was first measured at +1.71dBm. This signal was input directly into the ZHL-42 amplifier. Output power was measured from amplifier at +36.51dBm. The next power measurement was taken on each individual line at the connector to each AD8346EVAL CCA, after passing though the 24-way power divider and along each two-foot section of T-FLEX wave-guide. Power out from the amplifier was attenuated 6.0dBm to ensure final input to the AD8346EVAL was less than +10dBm. Measured input power to each AD8346EVAL was 9.96dBm.

3. AD8346EVAL Quadrature Modulator CCA Phase Accuracy Verification Digitally via LabVIEW Control Program

This calibration was a repeat of the bench test conducted previously to verify the phase shifting capability of the AD8346EVAL CCA. Using the LabVIEW control program, manual phase shift values were entered in five-degree increments for one AD8346EVAL CCA. Phase accuracy was measured with the VNA. Average phase accuracy was calculated at $1.20°$. Results are

summarized in Table 3 below.   Random spot-checks of some the
other AD8346EVAL CCA's returned similar results.   Table 5
lists the results for element one's "phase shifter".

PHASE INPUT	VNA MEASUREMENT	ERROR
000	-000.6	-0.6
015	015.9	+0.9
030	031.8	+1.8
045	045.8	+0.8
060	059.1	-0.9
075	073.2	-1.8
090	088.7	-1.3
105	105.9	+0.9
120	122.1	+2.1
135	136.4	+1.4
150	149.8	-0.2
165	165.1	+0.1
180	179.8	-0.2
195 (-165)	-163.3	-1.7
210 (-150)	-147.4	-2.6
225 (-135)	-133.6	-2.4
240 (-120)	-120.5	+0.5
255 (-105)	-106.7	+1.7
270 (-090)	-090.9	+0.9
285 (-075)	-073.8	-1.2
300 (-060)	-057.5	-2.5
315 (-045)	-043.2	-1.8
330 (-030)	-029.8	-0.2
345 (-015)	-015.8	+0.8
360 (000)	-000.5	-0.5
-015	-015.7	+0.7
-030	-029.8	-0.2
-045	-043.1	-1.9
-060	-057.5	-2.5
-075	-073.9	-1.1
-090	-091.0	+1.0

Table 5.   Digital Characterization of AD8346EVAL CCA

4.   Path Length Phase Error Calibration

Every LO signal pathway from power divider to dipole
antenna element had to be precisely calibrated.   Differences
in path length error translate into phase error at the
radiating dipole element.   This is a crucial factor since

53

phased array radars require both accurate and precise phase control for proper beam-forming operation.

The VNA was used to emulate the LO signal at 2.398340GHz and connected just prior to 24-way power division. Each AD8346EVAL card was set via the LabVIEW control program at 000.0° phase shift, which corresponds to a value of 1.000 VDC applied to each IP control pin. Element one was used to calibrate the VNA and set at zero phase error. All other elements are referenced to element one. Connecting the VNA individually to each AD8346EVAL VOUT at the point where the T-FLEX cable mates with the dipole antenna element, each element's phase error was measured and tabulated. Appendix G lists the data measured during this test. These figures are the values of the phase "offsets" used in the LabVIEW control program.

5. Dipole Element Return Loss Characterization

The twenty-four dipole elements were custom designed by Professor David Jenn and fabricated by Cirexx Corporation with a nominal operating frequency of 2.40GHz. Using the VNA, the return loss was measured for each of the elements. The best operating frequency would have been 2.46GHz with a return loss of −46dB. Maximum reflection allowed is −15dB, which corresponds to a reflection coefficient (R) of approximately three percent. The return loss of the worst element measured at −22dB and the best at −29dB at the specified operating frequency of 2.40Ghz (2.398GHz actual frequency). The calculated R at −22dB is less than one percent (0.67%), which is more than an acceptable return loss. Figure 21 displays

54

the VNA plot of the return loss measured for all twenty-four elements.
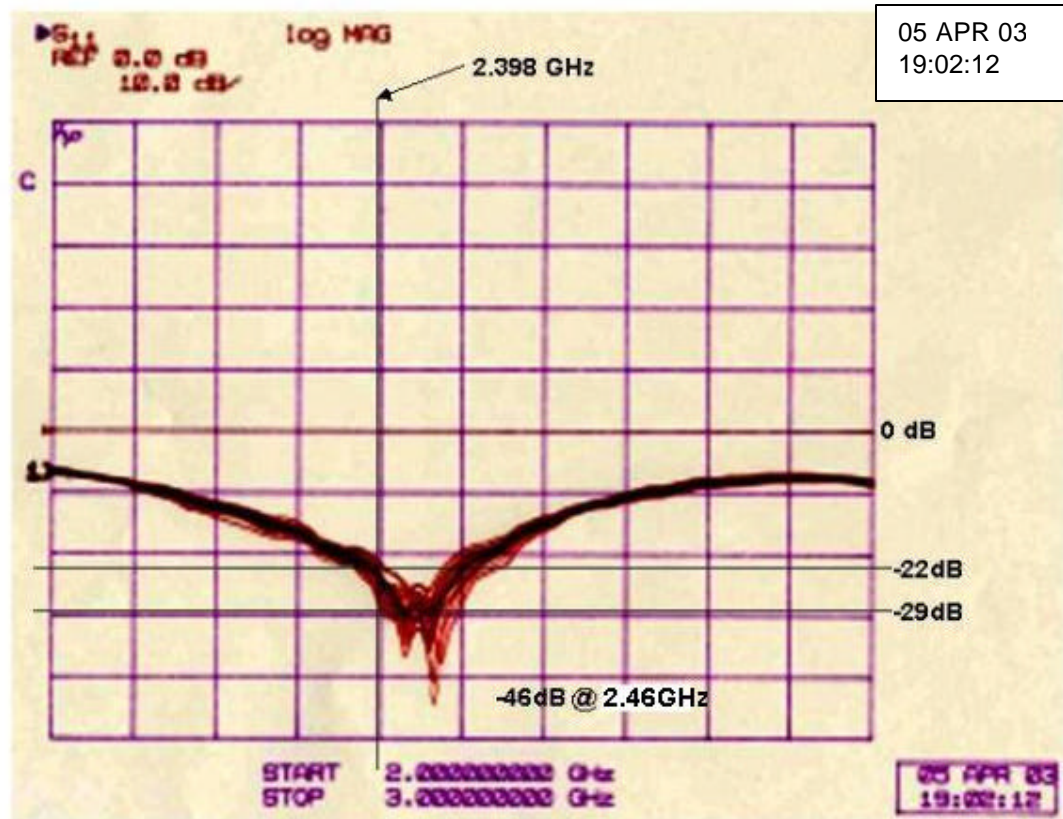
Figure 21: Dipole Element Return Loss

6.   Two Element Qualitative Analysis

To qualitatively characterize the system to this point, two dipole elements were mounted in a simple back plane. Using elements one and two, the VOUT cables were attached to the dipoles, mounted $l/2$ apart. Applying the measured offset to element two (remember element one is the reference phase), and zero phase shift, a beam was formed.   The beam maximum

power was measured using the HP E4419B EPM Series Power Meter connected to a 2.4GHz micro-strip antenna. By keeping standoff distance constant, and moving the antenna on a semi-circular arc, it was possible the measure main beam power. Main beam power was measured at 7-10 dB above sidelobes, and power fell off sharply outside beam pattern. A phase shift was introduced on one element, and then the other. In both cases, the main beam shifted to the appropriate direction, and power pattern measured was the same, just shifted as desired. This simple experiment validated the component operability to generate the LO signal, route it to the elements, control offset and phase via LabVIEW program, and the move beam center in the direction desired.

F. ANECHOIC CHAMBER MEASUREMENTS

1. Array Setup and Initialization

After situating the array and equipment cart in the anechoic chamber, some initial checks were conducted prior to taking actual radiation measurements or "cuts". After positioning the array on the pedestal in the chamber, the equipment cart was positioned behind it. Then the AD8346EVAL VOUT T-FLEX cables were connected to their respective dipole elements on the array. Initiating the embedded processor and radiating all elements with zero phase shifts, power measurements were taken with the HP E4419B EPM Series Power Meter and a simple 2.4GHz antenna. This verification was made to ensure that every element was in fact radiating. Using the same power meter and antenna, side and rear radiation leakage

measurements were taken. All measurements showed readings of −60dBm of lower. This was assumed to be of negligible impact.

Next, the VNA in the anechoic chamber was connected in place of the LO in the cart. This was required to allow the VNA to compute the readings at the receive feedhorn relative to the LO signal generated from the VNA. LO frequency was tuned to 2.398340GHz. Power out from the VNA was tuned to ensure that the input power to the AD8346EVAL CCAs did not exceed +10dBm. A Communications Corp. model HD 18565-feedhorn antenna was used for signal reception. Beam patterns for the boresight beam were measured to ensure the beam forming process was working. A boresight beam was detected and main lobe qualitative measurements were made by simple rotation of the pedestal. Main beam to sidelobe difference was approximately 10dB with a beam with of $10-15°$.

2.   Anechoic Chamber H-Plane and E-Plane Measurements

Beam forming measurements were taken in two planes, H-Plane and E-Plane. The H-Plane is perpendicular to the dipole axis while and the E-Plane parallel to the dipole axis. Coincidently, the H-Plane is also the horizontal or azimuthal plane, and the E-Plane that for elevation. This is because the antenna is vertically polarized. These fields would be reversed in a horizontally polarized antenna.

With the array situated atop the chamber pedestal, the feedhorn was located 19.0' away at a height of 56.0" to match the exact center of the antenna array. Alignment verification

was completed to ensure the zero position of the pedestal was aligned with the zero position of the antenna. Three sweeps were then conducted corresponding to GA runs LE13, LE19, and LE20 from Table 2. The boresight beam position LE13 was completed first, followed by LE19, which steered the beam horizontally $10°$ toward the –x direction, and finally LE20, which steered the beam $10°$ in the +x direction. With the phase files stored within the PXI-1042 embedded controller, changing beam direction took less than one minute. All H-plane measurements were taken in sweeps from $-60°$ to $+60°$ with $0.2°$ and 0.001dB resolution. Sweep sector size was limited to these values due to cable length and array size.

Once H-plane measurements were complete, the array was turned on its side, and braced to center the beam in the direction of the feedhorn. The feedhorn was rotated to match the transmit polarization and its height was adjusted to 58.50" with distance remaining at 19.0'. Array was realigned to pedestal center. Sweep sector sizes were limited at $-40°$ to $+40°$ also with $0.2°$ and 0.001dB resolution. Again, cable length and array size limited the range of angles. In both configurations, the feedhorn was rotated ninety degrees to check for cross-polarization of the fields. In all cases, this field was not readily measurable (less than -85dB). The E-plane measurements were taken in the same order as those for the H-plane.

G.   ANECHOIC CHAMBER DATA ANALYSIS

Data measured in the anechoic chamber was plotted and compared against that predicted by both the GA and the MoM calculations. The entire focus of this project was to prove the GA pattern builder function forms the same beam as predicted by the MoM method, which is a widely accepted means for computing phased array patterns. The MoM technique solves Maxwell's Electric Field Integral Equation. The antenna surfaces are separated into small sub-domains and the current on all of these regions is solved for simultaneously using matrix analysis techniques. These regions are assumed short if their length is small as compared to radiated wavelength and thus leads to a converged solution. This insures accurate current throughout the regions. The flat plates of the antenna are also divided into sub-domains that are small compared to the wavelength. These computed currents on the array surface are then integrated to determine the fields at any point in space using the principle of superposition.[3]

Figure 22 shows the antenna placement in the anechoic chamber for taking H-Plane data. Due to problems with jitter in the anechoic chamber's pedestal, some of the data was rough and disjoint. Professor David Jenn applied a MATLAB smoothing function to improve the presentation of the data. Figure 23 shows the comparison of the raw data plotted against the smoothed. As can be seen from the figure, the integrity of the data remains uncorrupted. Figures 24-26 show the data for H-Planes of boresight (LE13), $10°$ toward −x axis (LE19), and $10°$ toward +x axis (LE20) respectively. The blue curve

represents actual measured data in the anechoic chamber. The
GA prediction and MoM calculations are shown in green and red
respectively. Note, the MoM calculations were figured for the
far field case only. A bias error in alignment of the antenna
and the pedestal was discovered in the H-Plane runs. A
systematic $1.5°$ error was measured and corrected for. Figures
27-29 show the same data with a $1.5°$ bias error correction
applied to the measured data curve.
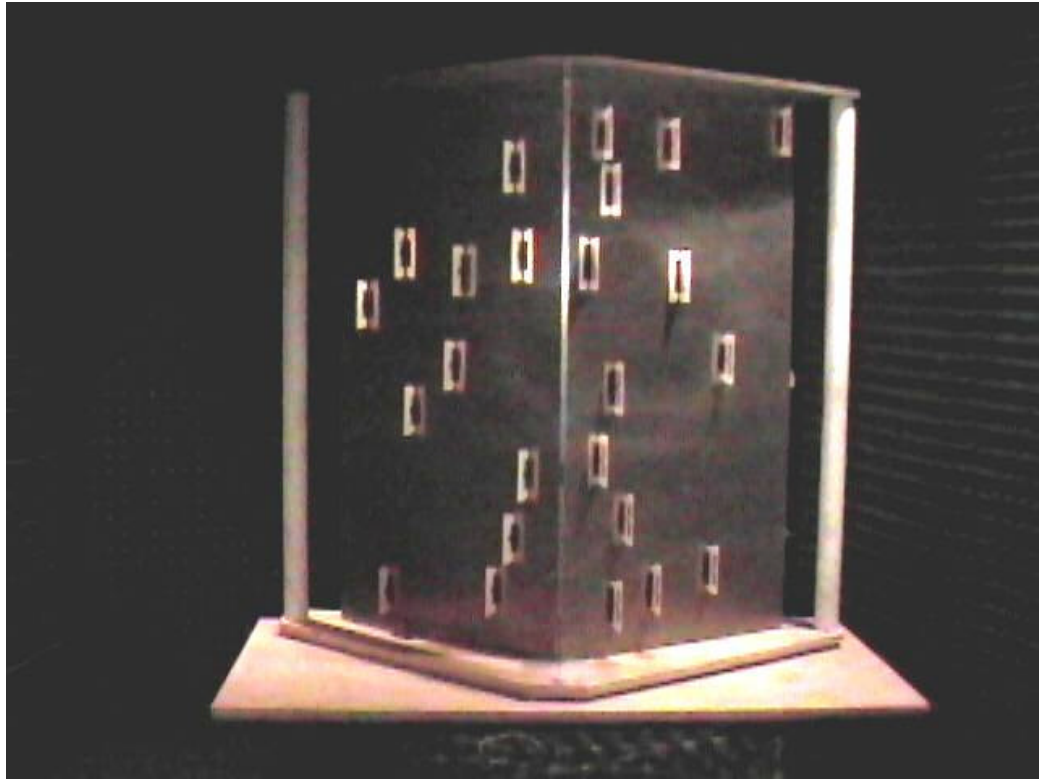
Figure 22: Antenna Placement for H-Plane Measurements
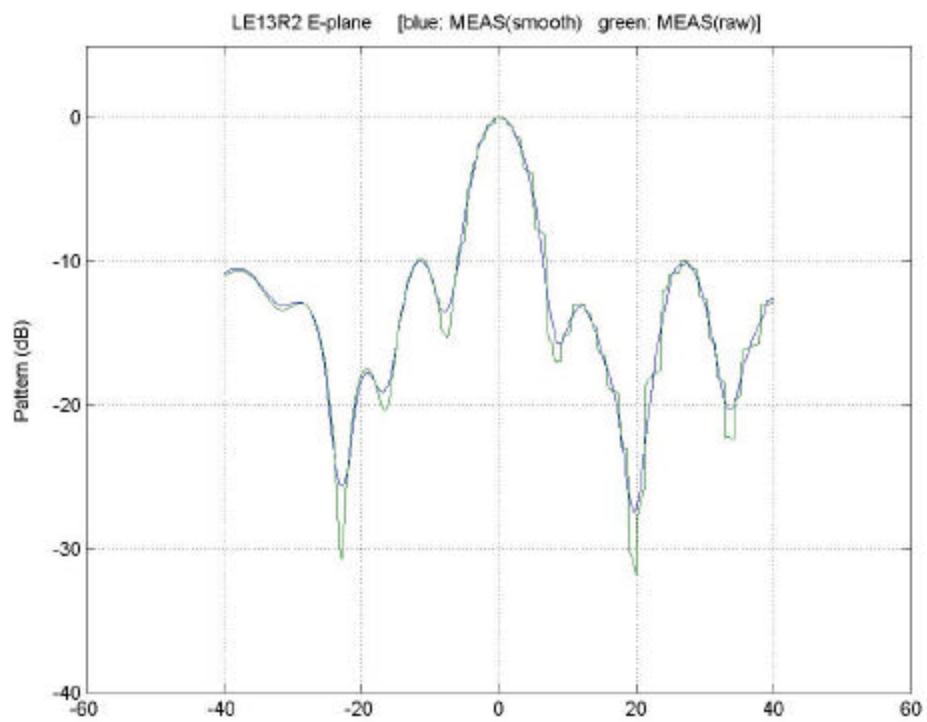
Figure 23: LE13 Raw Data versus Smoothed Data

61
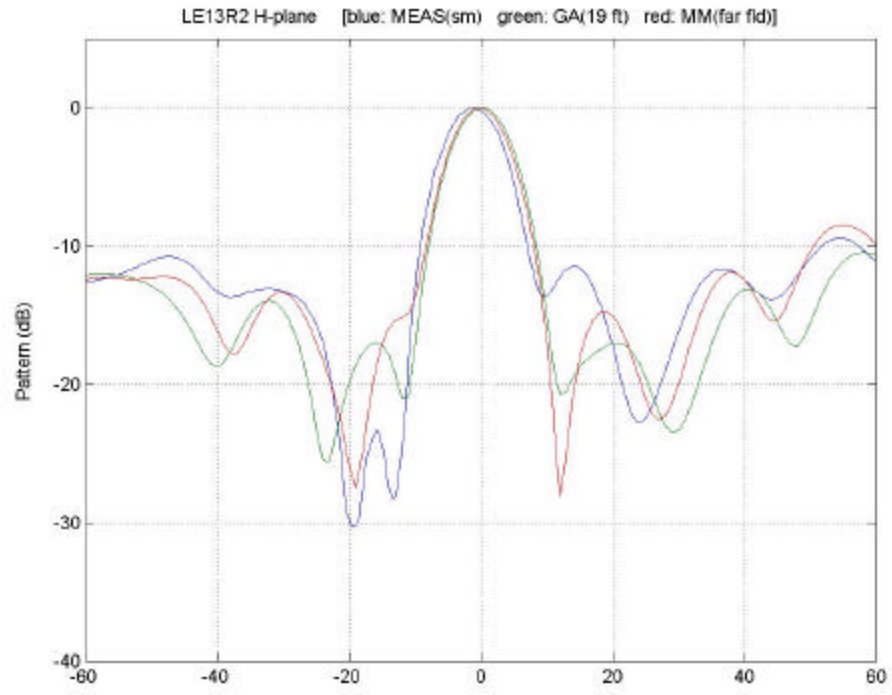
Figure 24: LE13 H-Plane

Figure 25: LE19 H-Plane

LE20R2 H-plane   [blue: MEAS(sm)   green: GA(19 ft)   red: MM(far fld)]
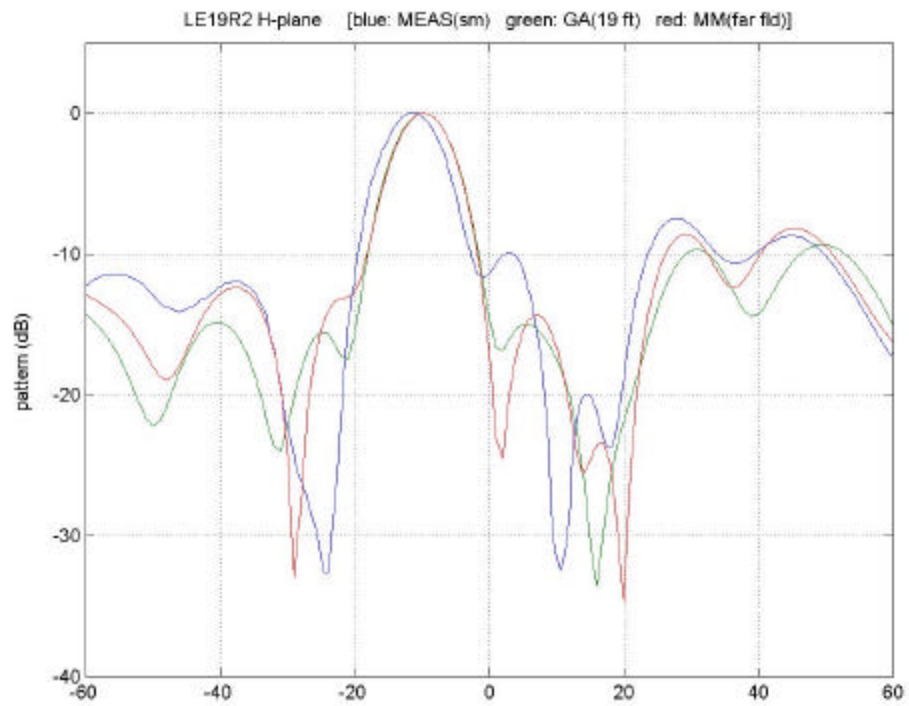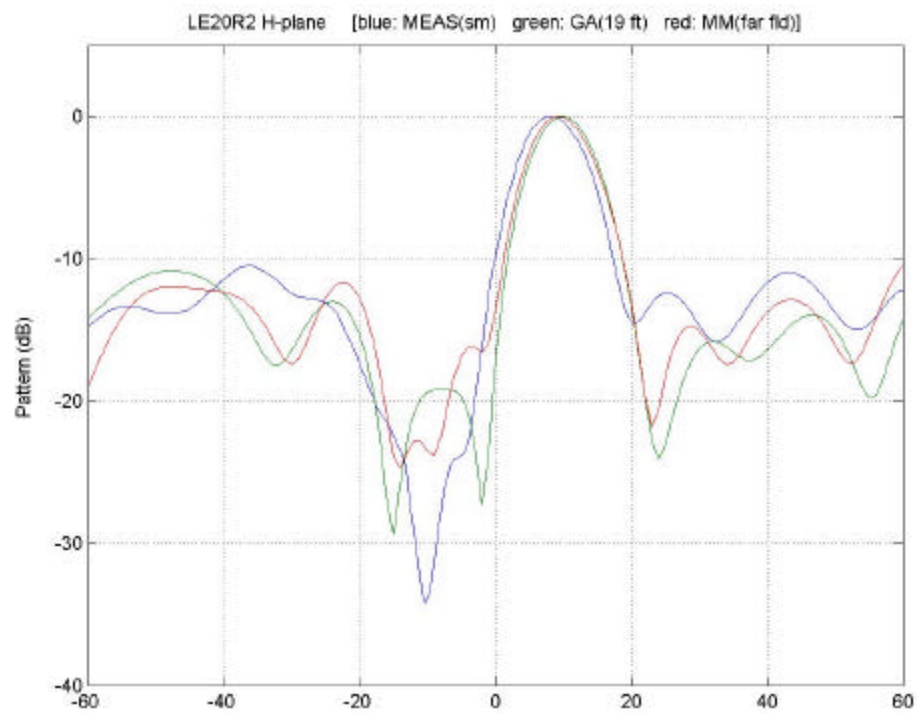
Figure 26: LE20 H-Plane
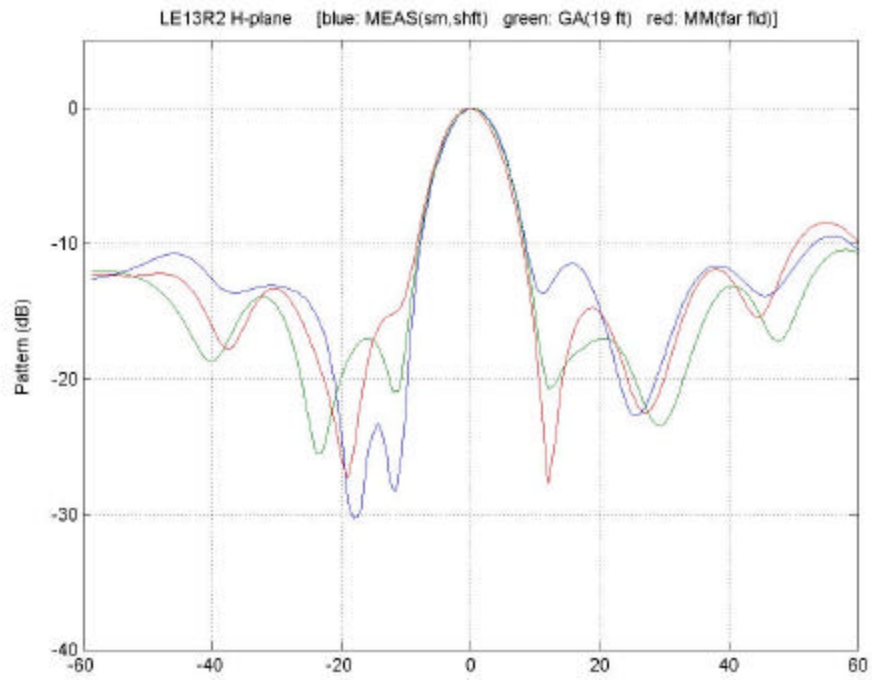
Figure 27: LE13 H-Plane Corrected for Bias Error
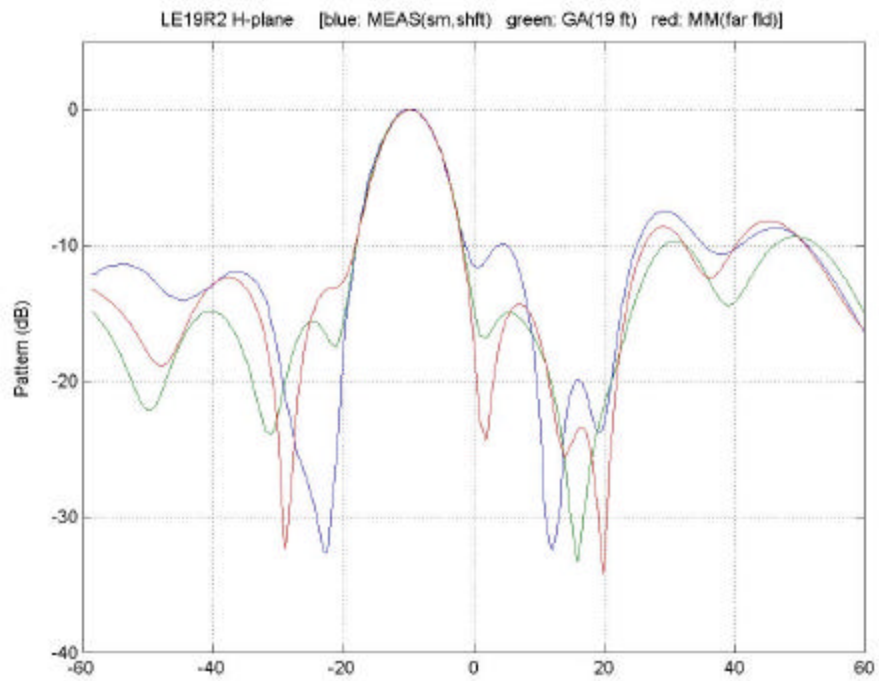
Figure 28: LE19 H-Plane Corrected for Bias Error

LE20R2 H-plane   [blue: MEAS(sm,shft)   green: GA(19 ft)   red: MM(far fld)]
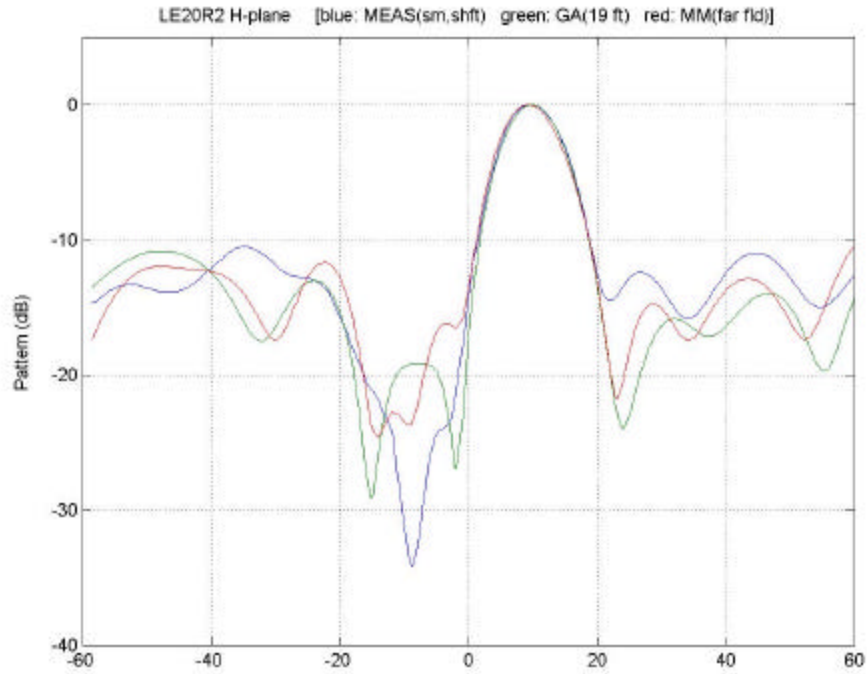
Figure 29: LE20 H-Plane Corrected for Bias Error

Figure 30 shows the antenna placement in the anechoic chamber for taking E-Plane data. Figures 31-33 display the E-Plane data. MoM calculations were not conducted for off axis E-Plane measurements.
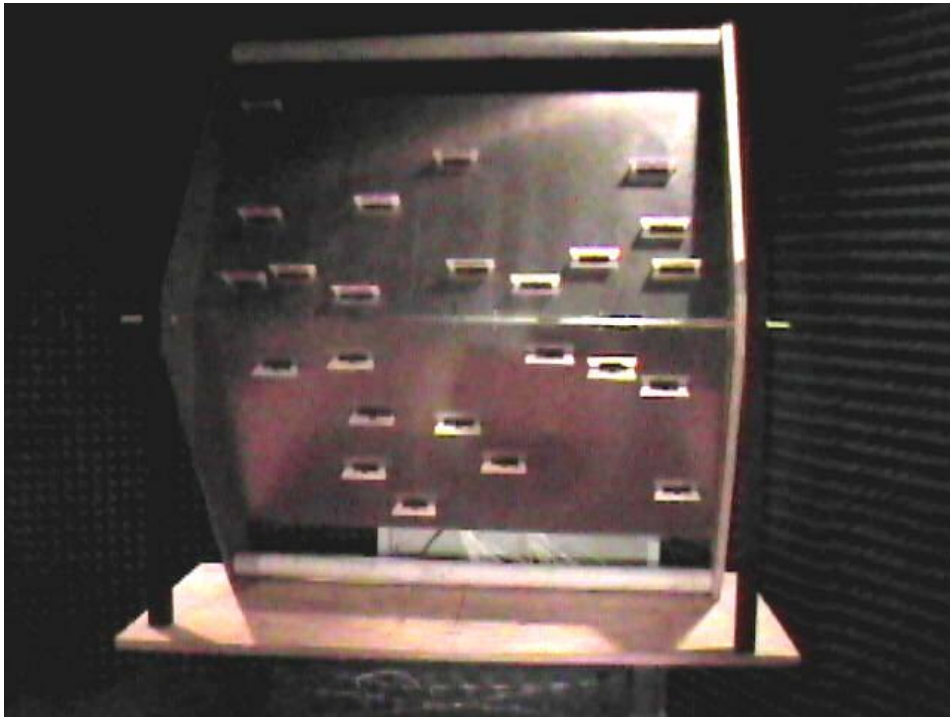
Figure 30: Antenna Placement for E-Plane Measurements
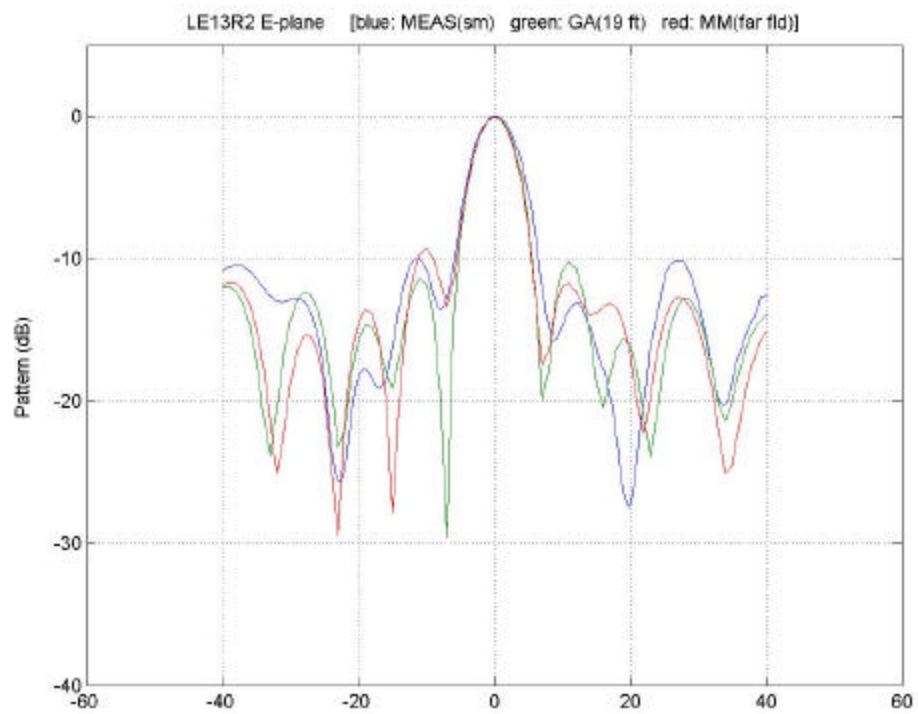
Figure 31: LE13 E-Plane
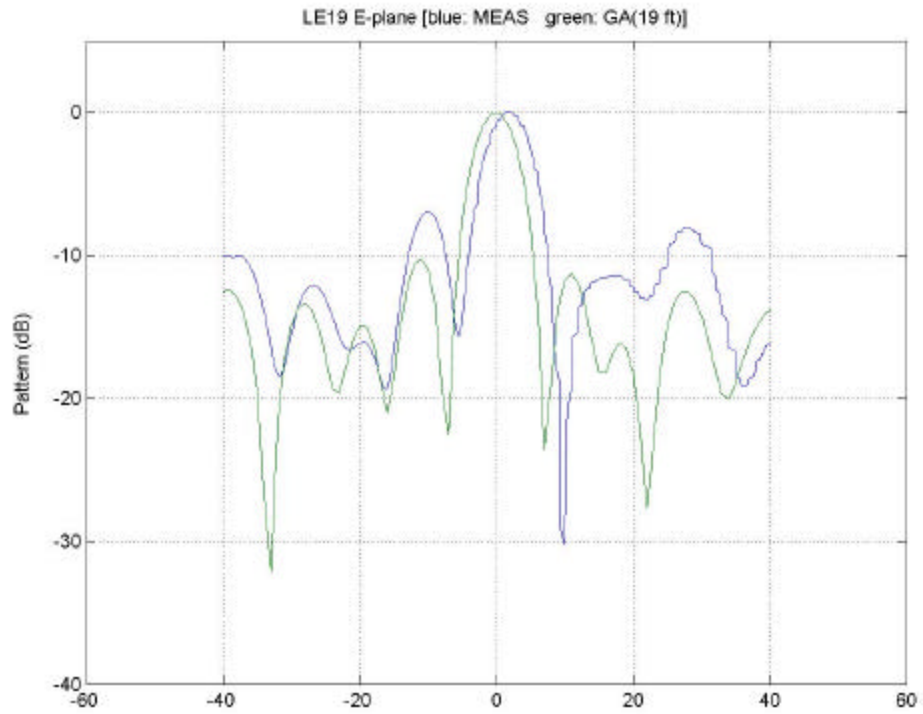
Figure 32 LE19 E-Plane
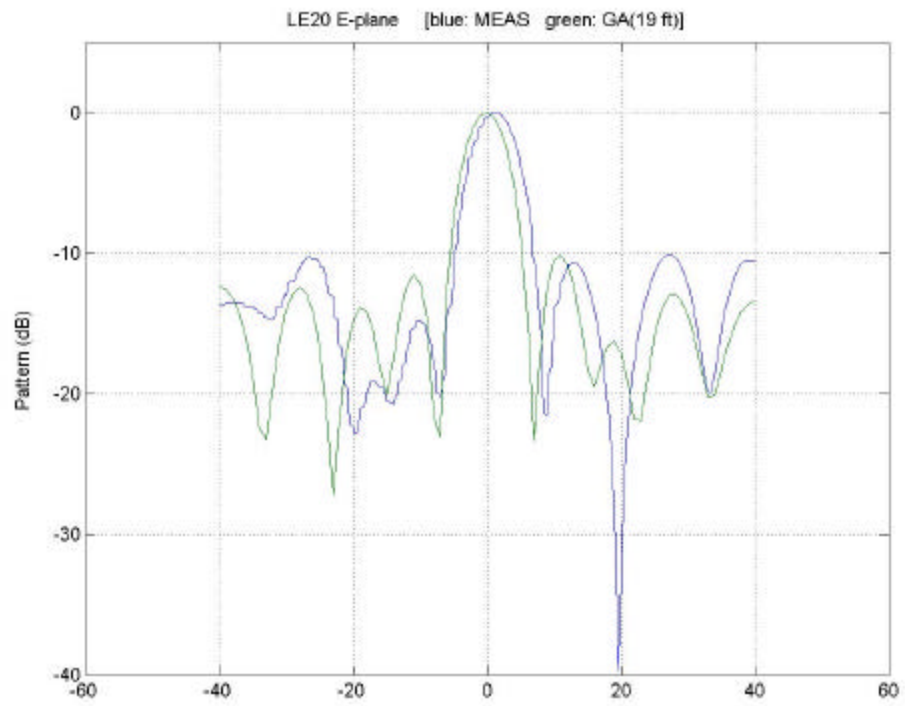
Figure 33: LE20 E-Plane

67

Considering the MoM calculations take into account all the interactions between elements as well as the edge effects, but the GA does not, data agreement is quite good. This validates the assumption within the GA model that these effects are negligible. Since main beam agreement between the sources is extremely close, it is obvious that the actual antenna is performing as the GA pattern builder predicted. The following principle observations are noted:

(1) There is a systematic bias error in alignment of the antenna centerline to feedhorn. This means that, without a benchmark, angular and positional alignment of the antenna with the pedestal centerline must be "eyeballed" for correctness. This error can be accounted for and adjustments made to the raw data.

(2) The anechoic chamber pedestal stepper motor was not functioning smoothly and appeared to be binding. This "jitter" caused jagged data recording. By using a MATLAB smoothing function, the data be realistically adjusted to better represent the actual shape of the beam pattern without compromising the integrity of the measured data.

(3) While the MoM calculation takes into account edge effects of the ground plane and inherent capacitive and inductive coupling between individual elements, the GA does not. In plotting the comparison of these two methods with the measurements, it is apparent that these effects are negligible.

(4) Neither modeling program accounts for the presence of the pedestal antenna mounting structure. Reflections from the array structure may be the source of some of the error in the actual chamber data. Changing out the 1″ thick polycarbonate base plate to ½″ plywood appears to have reduced some of the errors associated in the trial data runs. Thus some of the variations in sidelobes and nulls may have been caused by the antenna's supporting hardware, by additional reflection and interference effects not modeled.

(5) The anechoic chamber conditions may have contributed to some error in the data. As documented in Bartee, there are some regions of the chamber that cause abnormal measurements. The chamber's asymmetric geometry (footprint) could result in unaccounted for interference. Wear around the door seals was a documented source of error in Bartee. The inability to insulate the equipment cart in the chamber could have similar effects.

(6) Maximum inherent phase error in the AD8346EVAL CCA's is $+/-2.5°$. Error could exist in path length on the dipole element resulting in additional phase error. Offset measurements were made up to the radiating dipole element, but including it.

THIS PAGE INTENTIONALLY LEFT BLANK

IV.   CONCLUSIONS AND RECOMMENDATIONS

A.   EXPERIMENTAL SUMMATION

The objective of this thesis was twofold. The first was to verify that the GA program and its pattern builder function would form a beam in agreement with the Method of Moments calculations. The second was to build a digital transmit phased array antenna from commercially available components. Both of these objectives were accomplished. Digital modulator boards were obtained and their electrical performance characterized. Laboratory investigations determined that the boards were capable of controlling both amplitude and phase, thereby making a completely digital antenna possible. The boards were assembled into a twenty-four element array that used printed circuit dipoles as the radiating element. Measurements in the anechoic chamber verified that the beam could be scanned. Overall, the measured patterns were in good agreement with the predicted. Differences between the two could be attributed to alignment and measurement system errors. Although the GA is capable of synthesizing a low sidelobe pattern, only phase scanning was used in this demonstration.

B.   RECOMMENDATIONS FOR FUTURE EXPERIMENTS OR PROJECTS

1.   Receive Antenna

The next step in the process is to develop the

complementary receive array. This would allow the GA to be verified for the entire beam forming process from transmission to reception. The receive array should also be a thinned array with randomly located elements of the same frequency and wavelength. It should allow for broadband or wideband applications as the transmit array will undoubtedly be upgraded with such capabilities. Three dimensional geometry capabilities should planned for, similar to current dual ground-plane antenna.

2. Amplitude Tapering

The GA can provide both amplitude and phase settings to control the beam pattern. Using the existing array, beam patterns with amplitude variation or "tapering" can be implemented. The current system is already configured for this capability. Amplitude tapering can be used to reduce sidelobe levels, which is required in a high performance radar.

3. Broadband Upgrade to Current Active Array

Follow on work is planned to upgrade the existing active three-dimensional array with a wideband waveform. The current AD8346EVAL CCA phase shifters can support the frequency range of 0.8-2.5GHz. Phase shifting accuracy would have to be verified through the entire frequency range. Post phase shift amplifiers will be needed to provide for viable output power. Current power out was adequate for anechoic chamber

measurements; however, it will not be sufficient for real world tracking experiments. Additional experiments include evaluating the capability for using multi-frequency wideband applications coupling both sensor and communications capabilities in the same array.

4. Distributed Aperture Arrays

The advantages of designing an array within the structural constraints of a given platform would be immense. Imagine the radar built into the airframe of the AWACS itself or into the entire superstructure of a warship. While this thesis just scratched the surface of three-dimensional arrays, the capability of designing arrays on uneven, disjoint, or even curved surfaces would be a great advantage in platform design. Using multi-frequency wideband applications coupling both sensor and communications capabilities in the same array, many war fighting advantages could be realized, including reduction in platform RCS and enhanced surveillance capabilities due to increase sensor surface area. The GA should be evaluated for its capabilities and limitations in this type of antenna geometry.

5. Spanagel Hall as a Wide Aperture Array

Using one side of Spanagel Hall (or any building for that matter) as a multi-frequency distributed array should be considered. Elements could be placed either at random or by GA evolution on the windows and roof of the building. This problem is closely related to distributed apertures on a ship.

However, there are ground-based applications where the side of a building could serve as an antenna. An example is the bistatic hitchhiker radar system called "Sentinal". Using both a radar tracking frequency and a communications band, aircraft flying into Monterey Airport, and boats in Monterey bay could be tracked. Separate air and surface radar frequencies should be used to demonstrate dual radar frequency capability as well as a band for simultaneous connectivity for voice and data transmissions. Accurate real time measurements of the element locations will need to be addressed to account for temperature and structural fluctuations. A similar problem is encountered on a ship on the high seas.

6. Comparison of GA vs. Other Synthesis Methods

In this application, the GA was used to synthesize the excitations required to form a beam with the desired radiation characteristics from known element locations. There are other synthesis methods that are available, for example, Woodward's technique or the Fourier Transform method.[1] The current literature suggests that the GA has advantages over the others when random geometries are involved. Research should be conducted to quantify the advantages.

7. Monopulse Beam Steering

The capability of the GA to create a monopulse beam and steer it to desired locations should be evaluated. Most high performance tracking radars use monopulse beams. Also this capability is crucial in combating an Electronic Attack or

jamming threat as well as countering the effects of interference. The null locations can be stipulated as one of the GA pattern constraints. This would lend additional support legitimacy of the GA as a radar design tool.

C.   RADAR DESIGN IN THE FUTURE

The Genetic Algorithm coupled with a completely digital antenna of the type demonstrated here has the potential to break the paradigm in traditional methods of shipboard sensor design. The GA and programmed digital hardware easily adapt to the ever-changing requirements of sensor geometry and performance. This thesis has proven but a small part of the GA capability as radar design tool. Future research will demonstrate the flexibility of the digital antenna, with fully functional transmit and receive antennas used to investigate new and innovative radar system designs and processing techniques.

THIS PAGE INTENTIONALLY LEFT BLANK

APPENDIX A: GLOSSARY OF TERMINOLOGY AND ACRONYMS

ADI	Analog Devices Incorporated
AWACS	Airborne Warning and Control System
CCA	Circuit Card Assembly
CDMA	Code Demand Multiple Access
COTS	Commercial Off The Shelf/Commodity Available
DAC	Digital-to-Analog Converter
dB	Decibels
dBm	Decibels relative to 1 milliwatt
DCS	Digital Cellular Service
EA	Electronic Attack (Jamming)
FAD	Fleet Air Defense
fitness	Computed quantifiable score of the effectiveness of a population member as a solution to the given problem
GA	Genetic Algorithm
GHz	Gigahertz (10^9 cycles/second)
generation	A complete GA reproductive cycle including evaluation of fitness, selection and the formulation of a new population for the next generation.
GSM	Groupe Speciale Mobile, Global System for Mobile Communications
helipot	Helicoil Potentiometer
HP	Hewlett-Packard
individual	A discrete set of bit strings and/or vectors that forms a complete solution to the given problem as evaluated by the fitness function.
IEEE	Institute of Electrical and Electronics Engineers
ISAR	Inverse Synthetic Aperture Radar
ISM	Industrial, Scientific, and Medical
λ	Lambda – Wavelength
LCS	Littoral Combat Ship
LO	Local Oscillator
MFAR	Multi-Function Array Radar
MHz	Megahertz (10^6 cycles/second)

MoM	Method of Moments
NCTR	Non-Cooperative Target Recognition
NI	National Instruments
f	Phi – Phase
PCS	Personal Cellular Service
population	All the individuals in a given GA run
QAM	Quadrature Amplitude Modulation
QPSK	Quadrature Phase Shift Keying
RCS	Radar Cross Section
RF	Radio Frequency
RFIC	Radio Frequency Integrated Circuit
ROE	Rules of Engagement
SAR	Synthetic Aperture Radar
SARTIS	Shipboard Advance Radar Target Recognition System
SUW	Surface Warfare
TBMD	Theater Ballistic Missile Defense
TCP/IP	Transmission Control Protocol/Internet Protocol
TR	Transmit/Receive
TSSOP	Thin Sealed Small Outline Package
n	Nu – Frequency
UHF	Ultra-High Frequency
VDC	Volts Direct Current
VHF	Very High Frequency
VNA	Vector Network Analyzer

APPENDIX B: BASIC GENETIC ALGORITHM THEORY

A.   INTRODUCTION

The following review of basic genetic algorithm theory is an excerpt from: "Genetic Algorithms as a Tool for Phased Array Radar Design", Master's Thesis by Jon A. Bartee, LT, USN, June 2002. It is included an appendix for those not familiar with Phase One of the project and the Genetic Algorithm process.

A Genetic Algorithm proceeds through a succession of generations. Each generation is composed of a number of individual population members. These are vectors consisting of characterized traits that form a potential complete solution of the problem. The figure on the following page, displays the logical flow of solving a problem using a Genetic Algorithm.

Note in particular the loop structure. Each iteration of the loop is considered a generation. The relatively simple structure potentially allows several thousand generations of evolution to be completed in only a matter of hours with even modest computing resources. However, as a practical matter, the time it takes to complete a loop depends heavily upon how long it takes to do the fitness evaluation. Consequently, interesting problems that apply to real world needs often have a tendency to get bottlenecked computationally on the evaluation step. It should also be clear that the loop structure as shown would continue indefinitely until stopped
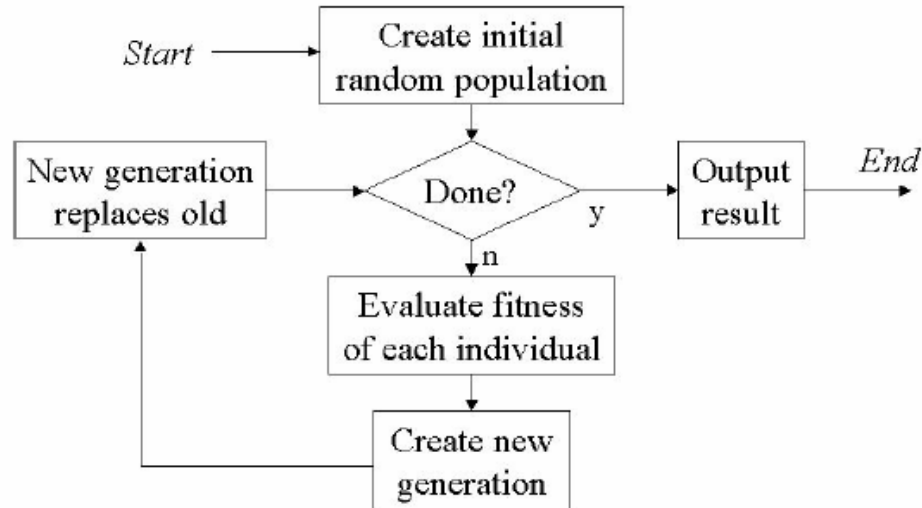
Figure 34: Genetic Algorithm Logic Flow (From Johnson, 15 August 2001[1])

in some way. The question of when to halt the evolutionary process is another consideration for the programmer.

"Fitness" is the criterion to be optimized and is the basis for selection of individuals from the population of each generation. The method used to evaluate the fitness of individual population members, as well as the four commonly used reproduction methods for determining the population of each generation will be covered in more detail.

B. MECHANISMS IN GENETIC ALGORITHMS

Genetic algorithms use several mechanisms to evolve a system over the course of the run. Selection of which mechanisms to use, and the probability each will have is a

critical decision for the programmer. Since Genetic
Algorithms are an iterative process, modeling either the
fitness criteria or individual incorrectly can cause the
program to diverge from answering the problem of interest to
the programmer. However, by self-correcting over the course of
a large numbers of these iterations, using assumptions and
criteria based on proven theory, the algorithm has the
capability of finding a set of most favorable solutions to
highly complex problems that might otherwise take years of
measurement and data collection.

1. Fitness Measurement

The initial item the programmer must address is how to
evaluate the traits of an individual population member against
the desired outcome. This is known as the "fitness
measurement," and it must be performed for each individual
during each consecutive generation of the run in order to be
able to faithfully rank the individuals' suitability to
deliver the desired result. Defining the fitness function is
the most critical step in the process. A failure to
effectively shape the question at hand in a form that can be
translated through a programming language into a measurement
of fitness for each individual relative to each other prevents
the preferential treatment of the best- suited individuals to
the next generation. This allows too many of the weaker
members to move on and the population will continue to be
characterized by randomness. Also important is the shaping of
the fitness criteria based on the reality of the problem. In
using a Genetic Algorithm to design and optimize an electrical
or mechanical system for example, the actual performance

parameters and physical limits of such a system must be faithfully reflected in the mathematics used to determine the relative ranking of the individuals. Without this fidelity to the physical world you might very well get an optimized solution to the problem posed, but that problem might not reflect the true complexity of the environment it must exist in and is therefore useless as anything other than an academic exercise. The fitness calculation may therefore be of a very complex nature.

The process is twofold. The fitness of each individual must first be evaluated and compared to its peers, and then individuals must be selected for a new population. The traits for each population member are evaluated using the fitness criteria, usually involving an analytic or numerical evaluation of a mathematical formula. The criterion must provide enough resolution that two individuals will usually have different values in order to be able to rank the entire population.   For example, in the case of a simple radar antenna design problem, the fitness assessment might involve determining the antenna gain for each individual. The traits of the individual might be those elements of gain, which are under the control of the designer: radar frequency, the antenna aperture efficiency, which is controlled by antenna shape and the physical area of the antenna.   The fitness assessment for each member would involve using the member's traits to calculate antenna gain in decibels, G_{dB}:[2]

$$G_{dB} = 10\log\left[\frac{4\boldsymbol{pr}_a A\boldsymbol{n}^2}{c^2}\right]$$

The value of r_a represents the antenna aperture efficiency, which is controlled by the physical shape and actual area, A, of the antenna.   Operating frequency is denoted by f and the speed of light by c.

The resulting gain would allow the individuals to be ranked from most fit, meaning highest gain, to least fit. Note that the fitness criterion is not expressed as a set binary limit, such as "above 30 dB," as this limits the ranking of individuals to only two categories.

2.   Population Selection

The population of any GA is composed of individuals. Each individual has discrete traits that characterize the individual and are directly applicable to the mathematics involved in determining fitness.   Generally speaking, the initial population is determined randomly for the first generation, and by the fitness assessment, selection, and creation of new individuals in subsequent generations.

a. Seeding

A refinement to population selection is the Concept of "seeding" the initial population of a Genetic Algorithm with the results of a previous run or predetermined configurations that represent probable solutions based on known facts, problem solver experience or even the best ranked results from previous runs.   Not only does the introduction of evolved, known or probable solutions cause more rapid

convergence, but it also allows the GA to be adjusted between runs in order to better track toward the desired goal.

b. Fitness- and Rank-Proportional Selection

Once the fitness of each individual has been determined the following step in formation of a new generation involves selecting the individuals that will be allowed to contribute genetic material to the next population through one of the genetic operators, described in detail later. Individual population members are selected for membership in the next generation by their relative fitness ranking with one of several methods, two of which are described below. Sometimes, a probability of selecting less fit individuals over more fit ones is included to retain some of the diversity of the original population, but the more fit ones must always have a higher probability of selection in order for a solution to emerge. A broader population diversity will result in slower convergence to the solutions of a problem and will require more computational resources and time, but has a greater chance of arriving at a better and perhaps unanticipated solution.

Fitness-proportional selection means that the probability of an individual being selected for continuation is weighted based on its performance during the fitness evaluation. One common method for fitness-proportional selection involves the creation of "bins," one for each individual present in the population. The size, or length, of an individual's bin is proportional to its assessed fitness. A random number is generated within the value range of all the

bins, and the individual in whose bin this number falls is selected for inclusion in the next generation, after the application of a genetic operator. Like pitching pennies into cups of differing sizes, there is a finite probability of selection for any individual but the individuals with better fitness scores have a higher probability of selection.

Problems can arise with fitness proportional selection when the raw fitness score values of most of the individuals are close to each other. This is particularly evident in later generations of a run, where all the individuals have begun to converge on a narrow range of solutions. The method for fixing this problem is to use rank-proportional selection. In rank-proportional selection, individuals are ranked with an integer value based on their raw fitness score, from 1 for the least fit to the population size, *n*, for the most fit. They are again placed in bins, but the bin size is now proportional to the integer ranking. The highest ranked individuals have the largest bins and therefore the higher probability of selection. The figure below illustrates this difference.
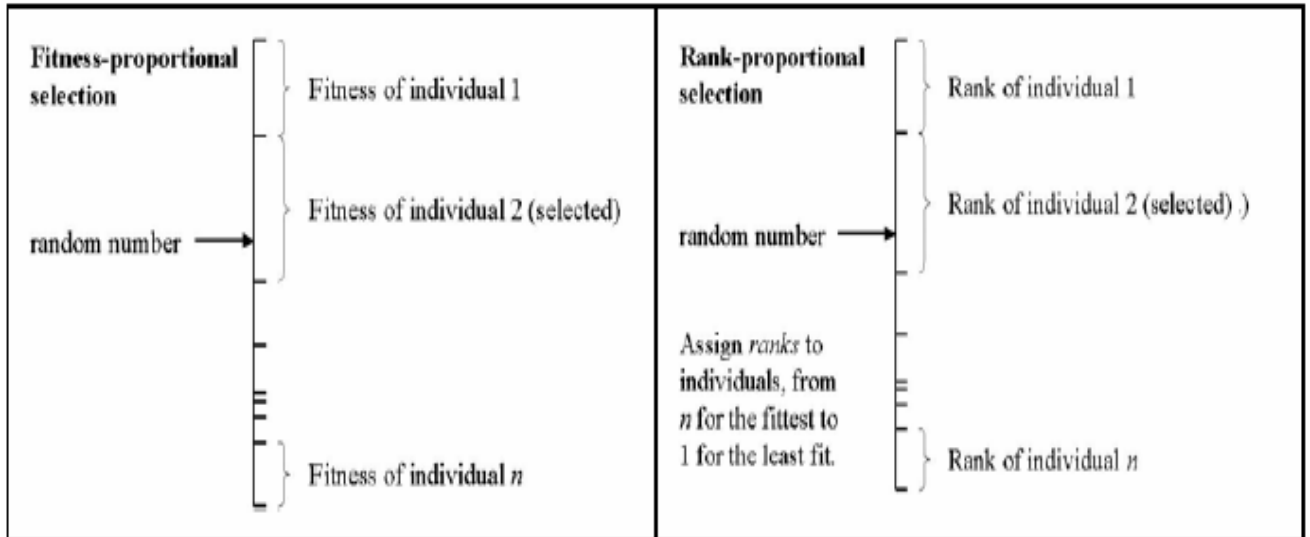
Figure 35: Fitness-Proportional vs Rank-Proportional Selection (From Johnson, 15 August 2001[3])

3.   Generalized Genetic Operators

Another item of concern to the writer of a genetic algorithm is the method by which individual population members will be used in creation of the next generation once their fitness has been ranked. There are four methods usually used for this process: reproduction, crossover, inversion and mutation, with each of the four having potentially independent mechanisms for determining if they occur. Each is normally assigned a probability of occurring, with this probability weighted in favor the individual's fitness ranking, thereby giving traits of the most fit the best chance of survival into later generations.   Using these four mechanisms, a new generation is formed and the fitness test is applied once again.

a. Reproduction

Reproduction, or the inclusion of an unaltered individual population member in the next generation is the simplest process of promotion for any Genetic Algorithm. The next figure shows the reproduction to a new generation graphically. When an individual population member is selected for reproduction the traits of the member, denoted as the vector a_1 through a_n in the figure below, are copied directly into an available slot for a population member in the new generation. No changes or rearrangements are made.
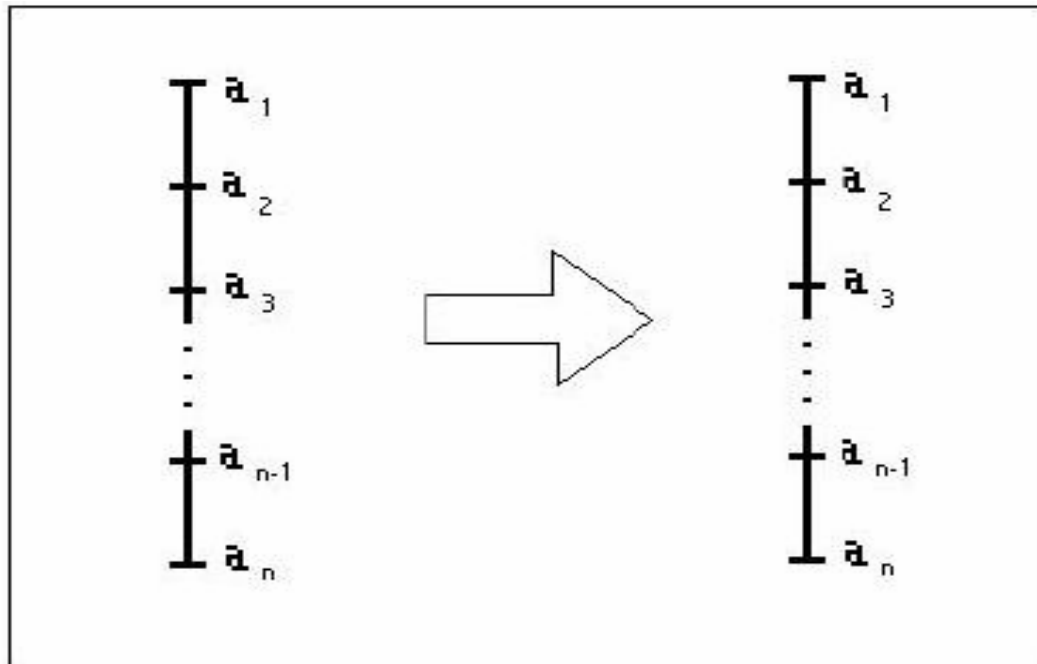
Figure 36: Illustration of Reproduction

The biological equivalent of this process could be seen as either survival of the individual or procreation through asexual reproduction, producing an identical copy of a single parent in the new generation. This mechanism is often assigned a significant probability of occurrence, although not

as high as crossover.   This same process is alternatively called copying or promotion.

b. Crossover

Crossover mimics sexual recombination in biological organisms. Starting with two parent members of the population, a number of distinct traits are swapped between mated pairs to produce two offspring, each different from the other and also from their parents, but with "genetic material" common to the family line.   Crossover is also controlled by probability, again usually weighted in favor of selecting more fit individuals as parents.   Like reproduction, crossover is usually assigned a relatively high probability of occurrence, usually exceeding the proportion assigned the other operators. The programmer must decide on values for some specific parameters that are not required for simple reproduction.   Two parents must be selected based on fitness, rather than one. The number of traits that will be crossed between mated pairs must be determined, and then a process must be included to determine which specific traits this will be.   The specific traits are often selected randomly to further promote innovative results.   The figure below shows an example of the crossover operation at work.
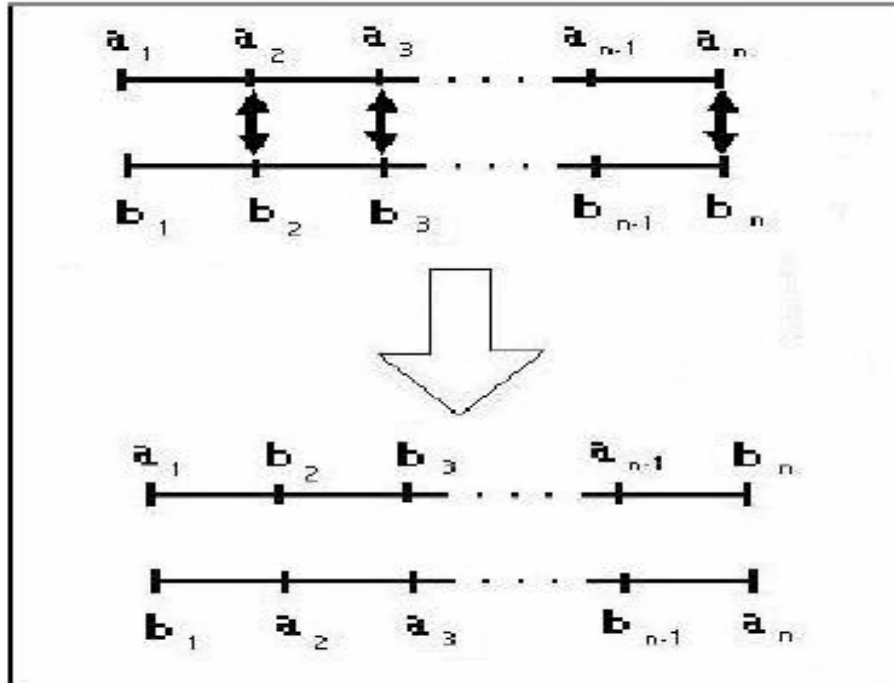
Figure 37: Illustration of Crossover

In the case shown in above, an individual with traits a_1 through a_n has been selected to mate with another member with traits b_1 through b_n. The programmer has chosen to use a three-point crossover, and traits with indices 2, 3 and n have been selected to be swapped between the parents. The resulting offspring are uniquely different from each other, and each is also different from both parents. Yet both share traits with parents who were more than likely to have been ranked higher than the average in fitness. Population members whose vectors schemes have few traits may be affected little by crossover operations.[4]

c. Inversion

Inversion is an unusual reproductive mechanism in

89

Genetic Algorithms, both for its effect on the selected population entity and because it really has no corollary in biological systems. If used at all, the probability of this type of genetic operation is often set very low compared to the previously mentioned cases. A single population member is chosen at random, again weighted toward the fittest individuals. Again, even numbers of random indices are chosen, usually two. There is no specific reason why only two points must be used for the process, but it keeps the operation simple and avoids unnecessary randomization of the traits. The vector is then effectively folded between traits with these two indices. This process is simplest to understand in illustration. A typical inversion operation is shown in the next figure.

Any possible rearrangement of traits can be accomplished by successive inversions. Also, like crossover, inversion has little effect on populations with individuals that have only a small number of character traits.[5]
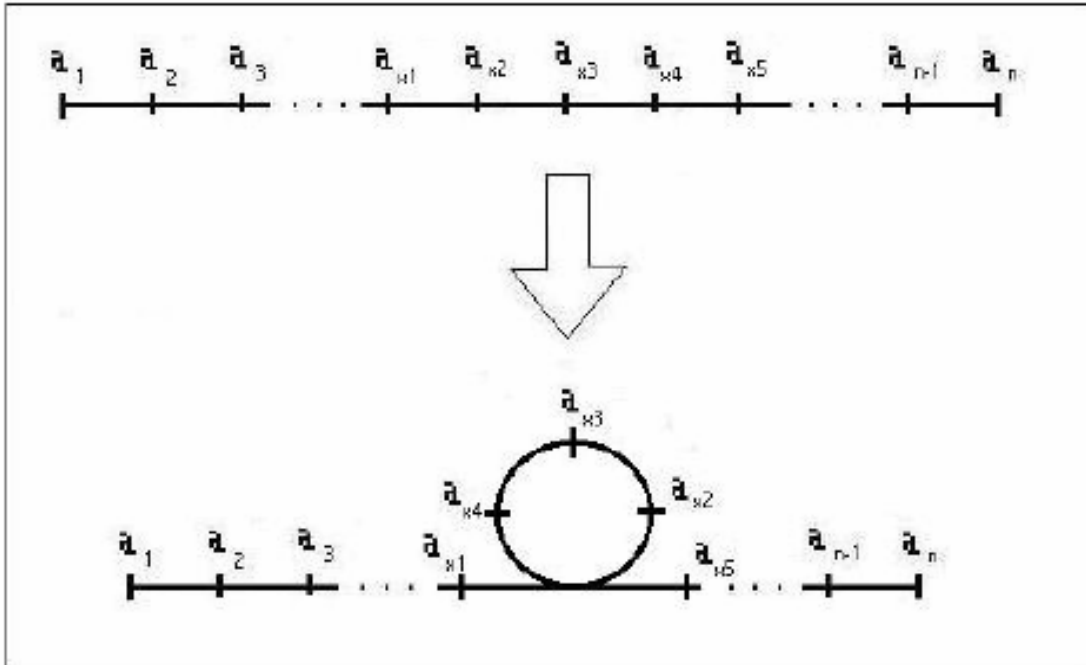
Figure 38: Illustration of Inversion (After Holland p. 107.[6])

d. Mutation

Mutation is another probability-controlled process which introduces random changes to the characteristics of an individual member, encouraging diversity in the population as a whole and therefore increasing the chances of a unique and otherwise unexpected solution. Directly analogous to the biological process of the same name, mutation can be easily applied in two distinct ways by the designer of a Genetic Algorithm. Either the probability mechanism can be applied the same way as with the other operators, with each individual having a set probability of a mutation somewhere in the individual's traits, with another random process determining which trait is effected, or in a more complex manner which can have a dramatically different effect. Unlike previous operators, arguably the most effective way to apply this genetic operator is by allowing an extremely small but non-

zero probability of a random change occurring for each trait in all individuals, rather than for the individual as a whole. The probability must be independent of whether mutation occurred in adjacent individuals, or even in an adjacent characteristic. This second method is undeniably more computationally intense. Traits selected for mutation are replaced with a random value within the designed limits of the attribute. The figure below shows the mutation process.
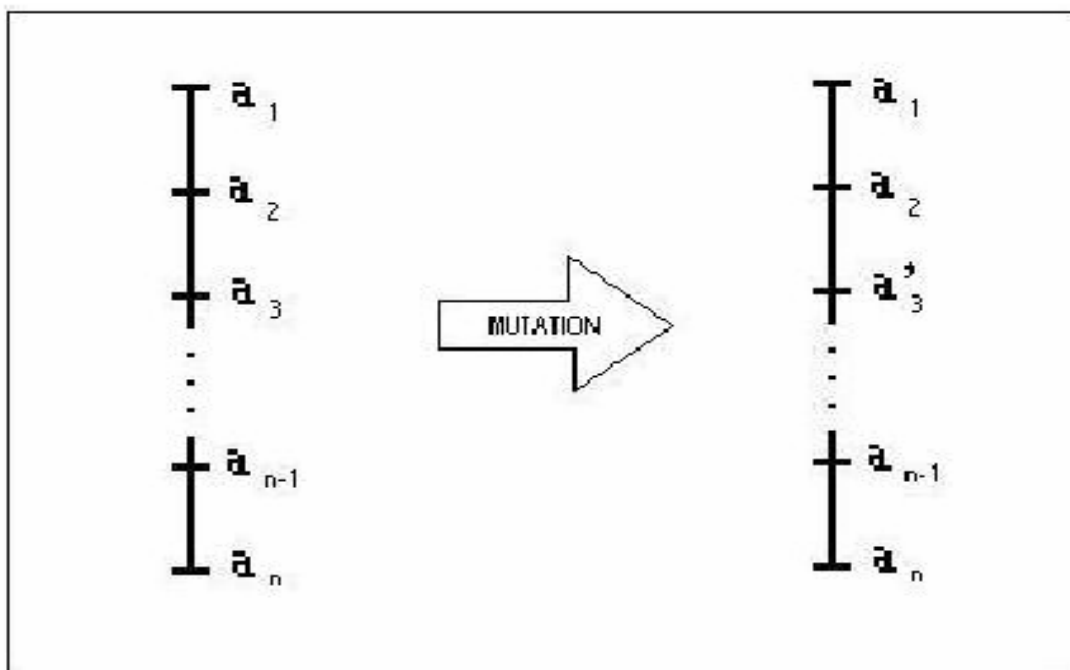
Figure 39: Illustration of Mutation

All the characteristic traits for this individual, as well as all other individuals in the population will independently be tested against a small operator-selected value for the probability of mutation. When a_3 is selected for mutation, a new trait value, a_3', is chosen at random to replace it in the new generation.

92

4. Stopping the Process

The final question that must be answered by the programmer is determining when to stop the process. If an exact solution is known, the code can be designed to stop on its own when it is achieved. However the use of a Genetic Algorithm in this case would be unnecessary! Computational constraints, such as programming language and hardware, are not only factors that limit population size, individual member complexity and fitness calculation intricacy, but also may limit the allowed run time on scarce computing resources. Genetic Algorithms will rarely arrive at an exact solution anyway, regardless of the amount of time allotted, due to embedded encouragement in the process for continued population diversity. The code may include a process by which an operator or the program itself may siphon off and observe the results of the process every few generations in order to determine if the algorithm is tracking in the desired direction or has achieved a solution that is good enough to be within set error limits for the task required. Either the programmer can then interrupt the process, or it may be programmed to jump out of the iterative loop. Other limiting factors may exist to curtail the run before the optimum solution is achieved, such as cost of constructing a physical device based on a Genetic Algorithm solution. By far the simplest way to end the run is to set a counter and run a pre-specified number of generations. At the end of these runs, the final output is all or part of the population of the final generation. Records may also be generated of previous generations, so that earlier sub-optimal solutions may be used

that keep materials, labor and complexity within the available budget.

APPENDIX C: MAJOR COMPONENT INVENTORY

COMPONENT	MANUFACTURER	MODEL# OR PART#	QTY	COST($)	TOTAL COST($)
Quadrature Modulator	Analog Devices Inc.	AD8346EVAL	24	99.00	2376.00
T-FLEX Microwave Cable 48"	SRC	SRC402SF	24	60.00	1440.00
T-FLEX Microwave Cable 24"	SRC	SRC402SF	24	60.00	1440.00
Low voltage signal cables IN,IP,QP,QN,PWUP	SRC	SRC316	120	25.00	3000.00
Power Divider 1x4	Meca Electronics	804-S-1.900-M01	1	193.24	193.24
Power Divider 1x6	Meca Electronics	806-S-1.900-M01	4	306.35	1225.40
Local Oscillator	Z-Comm	V800ME10	1	189.00	189.00
Amplifier	Mini-Circuits	ZHL-42	2	895.00	1790.00
Dipole antenna elements	Cirexx	N/A	24	1500.00	1500.00
DC Power Supply	Total Power International	T-40C	1	47.00	47.00
PXI-1000B 8 slot Chassis	National Instruments	PXI-1000B 777551-01	1	1777.50	1777.50
566 MHz Embedded Controller	National Instruments	NI-8174 778466-01	1	1615.50	1615.50
DC Analog Output and NI-DAQ	National Instruments	PXI-6704 777796-01	6	1255.50	7533.00
Cable Assy	National Instruments	SH-6868-D1 183432-01	6	112.50	775.00
Terminal Block	National Instruments	TBX-68 777141-01	6	1277.00	7662.00
AC Power Cord	National Instruments	763000-01	1	18.00	18.00

THIS PAGE INTENTIONALLY LEFT BLANK

APPENDIX D: ARRAY ELEMENT LOCATIONS

X lambda	Y lambda	X meters	Y meters
0.9867	-2.0463	0.1233	-0.2558
-0.8122	2.8014	-0.1015	0.3502
2.6987	0.1517	0.3373	0.019
-0.7587	-2.3243	-0.0948	-0.2905
-2.6306	-0.6499	-0.3288	-0.0812
0.8127	-3.2592	0.1016	-0.4074
-0.5255	-1.4169	-0.0657	-0.1771
-3.4751	0.8568	-0.4344	0.1071
3.7282	3.4745	0.466	0.4343
0.3427	1.4871	0.0428	0.1859
-2.7574	1.617	-0.3447	0.2021
0.7775	-0.2081	0.0972	-0.026
-0.6698	1.5946	-0.0837	0.1993
-1.8204	0.038	-0.2275	0.0047
1.5092	-3.0926	0.1886	-0.3866
1.8897	1.3278	0.2362	0.166
2.509	-2.904	0.3136	-0.363
0.5353	-1.1939	0.0669	-0.1492
0.6895	2.5003	0.0862	0.3125
-3.0297	-3.3727	-0.3787	-0.4216
-1.0561	-3.1206	-0.132	-0.3901
1.6611	3.1662	0.2076	0.3958
0.5352	3.2524	0.0669	0.4065
-1.6667	1.3779	-0.2083	0.1722

APPENDIX E: SYSTEM AND SUB-SYSTEMS SCHEMATICS

MASTER EQUIPMENT CONFIGURATION

120VAC POWER

NATIONAL INSTRUMENTS PXI-1042 CHASSIS W/566MHZ EMBEDDED CONTROLLER 6 X PXI 6704 DAC'S

6 X SH-6868-D1 DAC INTERFACE CABLES

TERMINAL BLOCK MOUNTING ASSY 6 X TBX-68

MONITOR

KEYBOARD

MOUSE

SRC-316 COAXIAL PHASE CONTROL SIGNAL CABLES

I N   I P   Q P   Q N

2.4GHZ SIGNAL

ZHL-42 AMPLIFIER

2.4GHZ SIGNAL

-6dB ATTENUATOR

2.4GHZ SIGNAL

24 WAY POWER DIVIDER

2.4GHZ SIGNAL

T-FLEX

ADI AD8346EVAL CCA

PHASE SHIFTED 2.4GHZ SIGNAL

T-FLEX

DIPOLE RADIATING ELEMENT

FREQ TUNING CONTROL

15VDC

V800ME10 LOCAL OSCILLATOR

5VDC CCA POWER

TYPICAL ELEMENT 24 TOTAL

5VDC

5 VDC POWER BUS

SWITCH BOX AMP/LO

5VDC LO POWER

15VDC AMP POWER

T-40C POWER SUPPLY

5VDC BUS POWER SUPPLY

120VAC POWER

CONTROL SIGNAL ROUTING

DAC2   DAC3   DAC2   DAC5   DAC6   DAC7

PXI-6704
DAC's NUMBERED
ACCORDING TO
CHASSIS SLOT
DESIGNATION

NI PXI-1042
CHASSIS W/
566MHz
EMBEDDED
CONTROLLER

SH-6868-D1
183432-01
CABLE ASSY

SH-6868-D1
183432-01
CABLE ASSY

TBX-68
TERMINALBLOCKS

TERMINAL
BLOCK BOARD
ASSEMBLY

TB2	TB5
TB3	TB6
TB4	TB7

24 IDENTICAL
CONFIGURATIONS

SRC-316
SIGNAL
CABLES

IP   QP

I N   Q N

ADI
AD8346EVAL
CCA

LOIN
INPUT
FROM LO
CKT

VOUT
TO DIPOLE
ELEMENT

PWUP
TO 5 VDC
POWER
SUPPLY

100

LOCAL OSCILLATOR SIGNAL SCHEMATIC

VNA
SIGNAL
SOURCE
SUPPLY

-6dB INLINE
ATTENUATOR

Z-COMM 24
GHz
V800ME10
Local
Oscillator

CHOICE OF
SIGNAL SOURCE

Mini-Circuits
ZHL-42
Amplifier

Meca Electronics
4-way Power Divider
804-s-1.900-MO1

+1.70 dBm
OUT

+30dBm
AMPLIFIER
OUT

PROVIDES ELEMENT CH
19-24

Meca Electronics
6-way Power Divider

PROVIDES ELEMENT CH
13-18

Meca Electronics
6-way Power Divider

PROVIDES ELEMENT CH
07-12

Meca Electronics
6-way Power Divider

CH 24

Meca Electronics
6-way Power Divider
806-s-1.900-MO1

PROVIDES ELEMENT CH
01-06

AD8346EVAL CCA
ELEMENT 01

DIPOLE
ELEMENT 01

CH 02

CH 01

Analog Devices
AD8346EVAL
Quadrature Modulator

24 ELEMENT OUTPUTS
to each
AD8346EVAL CCA

AD8346EVAL
LO IN@ +10dBm

DIPOLE
ELEMENT 02

Analog Devices
AD8346EVAL
Quadrature Modulator
(Phase Shifter)

Analog Devices
AD8346EVAL
Quadrature Modulator
(Phase Shifter)

TO: DIPOLE 24

POWER SUPPLY CONFIGURATION

0.5-4.5 VDC OUT
FREQ TUNING

1K OHM
FREQ TUNE
HELIPOT

Z-COMM 2.4GHz LO
V800ME10

ON/OFF
SWITCH

ON/OFF
SWITCH

MINI-CIRCUITS
ZHL-42 AMP

5 VDC
OUT

15 VDC
OUT

120 VAC
INPUT
POWER

TOTAL POWER INC
T-40C DC PWR SUP

AD8346EVAL
PHASE
SHIFTERs

ELEMENT 01

ELEMENT 02

5 VDC PWR
ELEMENTS 01-12

5 VDC
SUPPLY

5 VDC
TERMINALS
1 & 2
AD8346EVAL
PWR UP

.
.
.

ELEMENT 24

PXI-1042
CHASSIS W/
EMBEDDED
CONTROLLER

MONITOR
FOR
EMBEDDED
CONTROLLER

5 VDC PWR
ELEMENTS 13-24

120 VAC
POWER
SUPPLY

TERMINAL BLOCK PIN CONNECTIONS

Label	Pin	Pin	Label
+5V	1	35	DGND
DIO0	2	36	DGND
DIO1	3	37	DGND
DIO2	4	38	RFU
DIO3	5	39	DGND
DIO4	6	40	RFU
DIO5	7	41	DGND
DIO6	8	42	DGND
DIO7	9	43	AGND
ICH31[1]	10	44	VCH15
AGND15/AGND31	11	45	ICH30[1]
VCH14	12	46	AGND14/AGND30
ICH29[1]	13	47	VCH13
AGND13/AGND29	14	48	ICH28[1]
VCH12	15	49	AGND12/AGND28
ICH27[1]	16	50	AGND11/AGND27
VCH11	17	51	ICH26[1]
AGND10/AGND26	18	52	VCH10
AGND	19	53	ICH25[1]
AGND9/AGND25	20	54	VCH9
ICH24[1]	21	55	AGND8/AGND24
VCH8	22	56	AGND
ICH23[1]	23	57	VCH7
AGND7/AGND23	24	58	ICH22[1]
VCH6	25	59	AGND6/AGND22
ICH21[1]	26	60	VCH5
AGND5/AGND21	27	61	ICH20[1]
VCH4	28	62	AGND4/AGND20
ICH19[1]	29	63	VCH3
AGND3/AGND19	30	64	ICH18[1]
VCH2	31	65	AGND2/AGND18
ICH17[1]	32	66	VCH1
AGND1/AGND17	33	67	ICH16[1]
VCH0	34	68	AGND0/AGND16

ELEMENT#	CABLE#	SIGNAL	DAQ#	VCH#	PIN#	AGND#	PIN#
1	011	IN	2	0	34	0	68
1	012	IP	2	1	66	1	33
1	013	QP	2	2	31	2	65
1	014	QN	2	3	63	3	30
2	021	IN	2	4	28	4	62
2	022	IP	2	5	60	5	27
2	023	QP	2	6	25	6	59
2	024	QN	2	7	57	7	24
3	031	IN	2	8	22	8	55
3	032	IP	2	9	54	9	20
3	033	QP	2	10	52	10	18
3	034	QN	2	11	17	11	50

ELEMENT#	CABLE#	SIGNAL	DAQ#	VCH#	PIN#	AGND#	PIN#
4	041	IN	2	12	15	12	49
4	042	IP	2	13	47	13	14
4	043	QP	2	14	12	14	46
4	044	QN	3	15	44	15	11
5	051	IN	3	0	34	0	68
5	052	IP	3	1	66	1	33
5	053	QP	3	2	31	2	65
5	054	QN	3	3	63	3	30
6	061	IN	3	4	28	4	62
6	062	IP	3	5	60	5	27
6	063	QP	3	6	25	6	59
6	064	QN	3	7	57	7	24
7	071	IN	3	8	22	8	55
7	072	IP	3	9	54	9	20
7	073	QP	3	10	52	10	18
7	074	QN	3	11	17	11	50
8	081	IN	3	12	15	12	49
8	082	IP	3	13	47	13	14
8	083	QP	3	14	12	14	46
8	084	QN	3	15	44	15	11
9	091	IN	4	0	34	0	68
9	092	IP	4	1	66	1	33
9	093	QP	4	2	31	2	65
9	094	QN	4	3	63	3	30
10	101	IN	4	4	28	4	62
10	102	IP	4	5	60	5	27
10	103	QP	4	6	25	6	59
10	104	QN	4	7	57	7	24
11	111	IN	4	8	22	8	55
11	112	IP	4	9	54	9	20
11	113	QP	4	10	52	10	18
11	114	QN	4	11	17	11	50
12	121	IN	4	12	15	12	49
12	122	IP	4	13	47	13	14
12	123	QP	4	14	12	14	46
12	124	QN	4	15	44	15	11
13	131	IN	5	0	34	0	68
13	132	IP	5	1	66	1	33
13	133	QP	5	2	31	2	65
13	134	QN	5	3	63	3	30
14	141	IN	5	4	28	4	62
14	142	IP	5	5	60	5	27
14	143	QP	5	6	25	6	59
14	144	QN	5	7	57	7	24

ELEMENT#	CABLE#	SIGNAL	DAQ#	VCH#	PIN#	AGND#	PIN#
15	151	IN	5	8	22	8	55
15	152	IP	5	9	54	9	20
15	153	QP	5	10	52	10	18
15	154	QN	5	11	17	11	50
16	161	IN	5	12	15	12	49
16	162	IP	5	13	47	13	14
16	163	QP	5	14	12	14	46
16	164	QN	5	15	44	15	11
17	171	IN	6	0	34	0	68
17	172	IP	6	1	66	1	33
17	173	QP	6	2	31	2	65
17	174	QN	6	3	63	3	30
18	181	IN	6	4	28	4	62
18	182	IP	6	5	60	5	27
18	183	QP	6	6	25	6	59
18	184	QN	6	7	57	7	24
19	191	IN	6	8	22	8	55
19	192	IP	6	9	54	9	20
19	193	QP	6	10	52	10	18
19	194	QN	6	11	17	11	50
20	201	IN	6	12	15	12	49
20	202	IP	6	13	47	13	14
20	203	QP	6	14	12	14	46
20	204	QN	6	15	44	15	11
21	211	IN	7	0	34	0	68
21	212	IP	7	1	66	1	33
21	213	QP	7	2	31	2	65
21	214	QN	7	3	63	3	30
22	221	IN	7	4	28	4	62
22	222	IP	7	5	60	5	27
22	223	QP	7	6	25	6	59
22	224	QN	7	7	57	7	24
23	231	IN	7	8	22	8	55
23	232	IP	7	9	54	9	20
23	233	QP	7	10	52	10	18
23	234	QN	7	11	17	11	50
24	241	IN	7	12	15	12	49
24	242	IP	7	13	47	13	14
24	243	QP	7	14	12	14	46
24	244	QN	7	15	44	15	11

THIS PAGE INTENTIONALLY LEFT BLANK

APPENDIX G: PATH LENGTH PHASE ERROR CALIBRATION
(OFFSETS)

ELEMENT	OFFSET
	(PATH LENGTH ERROR)
01	000.0
02	072.8
03	046.3
04	103.4
05	101.8
06	082.8
07	048.5
08	093.2
09	096.1
10	051.6
11	035.1
12	019.4
13	039.5
14	008.6
15	043.9
16	037.6
17	075.3
18	040.5
19	086.7
20	119.7
21	034.4
22	030.8
23	003.5
24	061.3

THIS PAGE INTENTIONALLY LEFT BLANK

APPENDIX H: CABLE NUMBERING CONVENTION

Designation and identification of AD8346eval Quadrature Modulator cable connections. Using three digit numerical series, each cable is labeled according to the following convention:

XXX = XX Element Number 01-24 - X Cable ID   1 - IN
                                             2 - IP
                                             3 - QP
                                             4 - QN
                                             5 - 5 VDC PWUP

For example: 073 = AD8346 element #7, QP signal cable input.

Local Oscillator/AD8346EVAL VOUT T-FLEX cables ID labeled as follows:

XX = Element Number 01-24

THIS PAGE INTENTIONALLY LEFT BLANK

ENDNOTES

Chapter II:

1) Koza; (1992). *Genetic Programming*. Cambridge, MA: MIT Press. p. 17.

2) Copyright, Mathworks, Inc.

3) Jenn, David and Johnson, Rodney; "New Design Codes and Methods for Random-Element Phased- Array Antennas"; Presentation and slide show given at the United States Naval Postgraduate School for representatives of the Office of Naval Research (ONR); 13 March 2002.

4) Ibid.

5) Rao: (1991). *Elements of Engineering Electromagnetics, 3rd Edition*. Englewood Cliffs: Prentice Hall.

   Skolnik; (2001). *Introduction to RadarSystems, 3rd edition*. New York: McGraw-Hill. p. 562-3.

6) Griffiths; (1999)*Introduction to Electrodynamics, 3rd Edition*. p. 121-5.

7) Skolnik; (2001). *Introduction to RadarSystems, 3rd edition*. New York: McGraw-Hill. p. 562-3.

Chapter III:

1) Analog Devices AD8346 Data Sheet.

2) Ibid.

3) SETH Corporation (2002); *EMI/EMC Modeling Techniques – Method of Moments."* Retrieved at http://www.sethcorp.com/seth4.html

Chapter IV:

1) Balaris; (1982), *Antenna Theory: Analysis and Design.*

Appendix B:

1) From a slide presentation given by Dr. Rodney Johnson developed for the Institute for Joint Warfare Analysis (IJWA) at the US Naval Postgraduate School, "Phased-Array Antenna Patterns via Genetic Algorithms", on 15 August 2001.

2) Skolnik; (2001). *Introduction to RadarSystems, 3rd edition*. New York: McGraw-Hill. p 6.

3)   Johnson; "Phased-Array Antenna Patterns via Genetic Algorithms"; 15 August 2001

4)   Holland; (1992). *Adaptation in Natural and Artificial Systems*. Cambridge, MA: MIT Press. p. 97-106

5)   Ibid. p .107.

6)   Ibid. p .107.

LIST OF REFERENCES

Altschuler, E. and Linden, D. (1996). "Automating Wire Antenna Design Using Genetic Algorithms". *Microwave Journal*. March 1996. p 74-86.

Balaris, Constantine A. (1982), *Antenna Theory: Analysis and Design.*

Bartee, Jon A., LT, USN, *Genetic Algorithms as a Tool for Phased Array Radar Design,* NPS, June 2002.

Billetter, D. (1989). *Multifunction Array Radar*. Norwood, Massachusetts: Artech House Publishing.

Boas, M. (1983). *Mathematical Methods in the Physical Sciences*. New York: John Wiley and Sons.

Brandwood, D. and Baker, J. (1989). "*Stabilization of Adaptive Array Patterns Using Signal Space Projection." IEE Conference Publication 301, Pt. 1.*

Cantrell, B., de Graaf, J., Leibowitz, L., Meurer, G., Parris, C., Stapleton, R. and Willwerth, F. (2002). "Develepment of Digital Array Radar". *IEEE AESS Systems Magazine*. Volume 17. Number 3. March 2002. p. 22-27.

Chambers, L. (1995). *Practical Handbook of Genetic Algorithms: Applications Volume I*. New York: CRC Press.

Dorf, R. and Smith, R. (1992). *Circuits, Devices and Systems, 5th Edition*. New York: John Wiley and Sons.

Fogel, D. (2000). "What is Evolutionary Computation?". *IEEE Spectrum.*
February 2000. p. 26-32.

Giordano, N. (1997). *Computational Physics*. London: Prentice-Hall.

Griffiths, D. (1999). *Introduction to Electrodynamics, 3rd Edition*. London: Prentice-Hall.

Hecht, E. (1998). *Optics, 3rd Edition*. Reading, Massachusetts: Addison Wesley Longman Inc.

Holland, J. (1992). *Adaptation in Natural and Artificial Systems*. Cambridge, Massachusetts: The MIT Press.
Icheln, C., Ollikainan, J. and Vainikainan, P. (2001). "Effects of RF Absorbers on Measurements of Small Antennas in Small Anechoic Chambers". *IEEE AESS Systems Magazine*. Volume 16. Number 11. November 2001. p. 17-20.

Jacomb-Hood, A. and Purdy, D. (1999) "In Orbit Active Array Calibration for NASA's LightSAR". *IEEE Radar Conference*. Boston, Massachusetts: IEEE. p.172-176.

Jenn, D. and Johnson, R. (2002). *"New Design Codes and Methods for Random-Element Phased-Array Antennas"*. Presentation and slide show given at the US Naval Postgraduate School for representatives of the Office of Naval Research (ONR).

Johnson, R. (2000) *"Phased Array Antenna Patterns via Genetic Algorithms"*. Presentation by Professor Rodney Johnson of the Naval Postgraduate School.

Michielssen, E. and Weile, D. (1997). "Genetic Algorithm Optimization Applied to Electromagnetics: A Review". *IEEE Transactions on Antennas and Propagation*. Volume 45. Number 3. March 1997. p. 343-353.

Mitchell, M., Howard, R. and Tarran, C. (2002). *"Adaptive Digital Beamforming (ADBF) Architecture for Wideband Phased Array Radars." Georgia Institute of Technology Journal of Technology.* Georgia Institute of Technology.

Purdy, D. (2000). "Automated Process for Efficiently Measuring the Patterns of All Elements Located in a Phased-Array Antenna". *IEEE International Conference on Phased Array Systems and Technology*. pp. 521-524.

Kasap, S. (2002). *Principles of Electronic Materials and Devices, 2nd Edition*. New York: McGraw-Hill.

Koza, J. (1992). *Genetic Programming*. Cambridge, Massachusetts: The MIT Press.

Rao, N. N. (1991). *Elements of Engineering Electromagnetics, 3rd Edition.* Englewood Cliffs: Prentice Hall.

Reubens, P., ed. (2001). *Science and Technical Writing, 2nd Edition*. New York: Routledge.

Salter, D. (1988) *"MESAR: The Plessey/ARE Adaptive Phased Array Demonstrator." IEE Proc. Military Microwaves.* pp. 527-532.

Sanchez, E. and Tomassini, M. (1996). *Towards Evolvable Hardware: The Evolutionary Engineering Approach*. Berlin: Springer.

Skolnik, M. (2001). *Introduction to Radar Systems, 3rd Edition*. New York: McGraw-Hill.

Tarran, C. (1989). *"Adaptive Arrays: An Overview of QMC Antenna Symposium." Recent Advances in Antenna Theory and Design.* Edited by Clarricoats and Parini.

Willis, N. (1995). *Bistatic Radar*. Silver Spring, Maryland: Technology Service Corporation.

THIS PAGE INTENTIONALLY LEFT BLANK

INITIAL DISTRIBUTION LIST

1. Defense Technical Information Center
   Ft. Belvoir, Virginia

2. Dudley Knox Library
   Naval Postgraduate School
   Monterey, California

3. RADM David Altwegg, (ret.)
   Deputy Assistant Secretary of the Navy –
   Theater Combat Systems
   Washington, D.C.

4. CDR Billie S. Walden
   Program Executive Office – Theater Surface Combatants
   Washington Navy Yard
   Washington, D.C.

5. Dr. Thomas Kimbrell
   Naval Surface Warfare Center
   Dahlgren, Virginia

6. RADM Wayne Meyer, (ret.)
   W.E. Meyer Corporation
   Arlington, Virginia

7. CAPT Al Haggerty
   NAVSEA Code 426
   Washington, DC

8. Professor Michael Melich
   Wayne E. Meyer Institute of System Engineering
   Naval Postgraduate School
   Monterey, California

9. Professor David Jenn
   Department of Electrical and Computer Engineering
   Naval Postgraduate School
   Monterey, California

10. Professor Rodney Johnson
    Wayne E. Meyer Institute of System Engineering
    Naval Postgraduate School
    Monterey, California

11. Professor William Maier
    Chairman, Department of Physics
    Naval Postgraduate School
    Monterey, California

12. Professor Robert Harney
    Naval Postgraduate School
    Monterey, California

13. Dr. Dan Purdy
    Office of Naval Research
    Arlington, Virginia

14. Dr. Bobby Junker
    Office of Naval Research
    Arlington, Virginia

15. Nicholas Willis
    Carmel, California

16. Michael Cassidy
    Anteon Corporation
    Crystal City, Virgina

17. RADM Tim Hood, (ret.)
    Lockheed Martin Government Electronic Systems
    Moorestown, New Jersey

18. James Alter
    Naval Research Laboratory
    Washington, D.C.

19. Peter Wilhelm
    Naval Research Laboratory
    Washington, D.C.

20. Robert Eisenhauer
    Naval Research Laboratory
    Washington, D.C.

21. Ed Senasack
    Naval Research Laboratory
    Washington, D.C.

22. Professor Herschel Loomis
     Naval Postgraduate School
     Monterey, California

23. Dr. Ray Bernstein
     New Mexico State University
     Las Cruces, New Mexico

24. Professor Paul Moose
     Naval Postgraduate School
     Monterey, California

25. Professor Curt Schleher
     Naval Postgraduate School
     Monterey, California

26. Lee Hammarstrom
     Port Matilda, Pennsylvania

27. Lee Moyer
     Defense Advanced Research Projects Agency
     Arlington, Virginia

28. Michael Pollock
     Office of Naval Research
     Arlington, Virginia

29. Timothy Ehret
     Lockheed Martin Corporation
     Moorestown, New Jersey

30. Lieutenant Jonathon Garcia
     Naval Postgraduate School
     Monterey, California

31. Cher Shin Eng
     Naval Postgraduate School
     Monterey, California

32. LCDR Lance Esswein
     USS PIONEER(MCM-9)